CEPAS 2017

7th Conference on Elementary Processes in Atomic Systems

3rd – 6th September 2017

Průhonice, Czech Republic

Table of Contents

Local organizing comitee:

Václav Alt
Martin Čížek
Roman Čurík
Karel Houfek
Dávid Hvizdoš
Michal Tarana
Petra Votavová

International scientific committee:

Friedrich Aumayr, Austria
Joachim Burgdorfer, Austria
Robert DuBois, United States
Gustavo Garcia Gomez-Tejedor, Spain
Jiří Horáček, Czech Republic
Bratislav P. Marinkoviá, Serbia
Nigel J. Mason, United Kingdom
Ladislau Nagy, Romania
Zoran Lj. Petrović, Serbia
Otto B. Shpenik, Ukraine
Andrey Solovyov, Germany
Viorica Stancalie, Romania
John A. Tanis, United States
Károly Tőkesi, Hungary
Mariusz Zubek, Poland

Editors: Michal Tarana, Roman Čurík

First published: September 2017

Published by:

J. Heyrovský Institute of Physical Chemistry, v.v.i.
Academy of Sciences of the Czech Republic
Dolejškova 3, 18223 Prague 8
Czech Republic

ISBN 978-80-87351-46-8

Programme

Sunday, September 3

15:00		Registration
19:00		Opening and welcome reception

Monday, September 4

Photoionization and photoemission - *Chairman: Bratislav Marinković*

9:00	Fernando Martín	Attochemistry: Imaging and controlling electron dynamics in molecules *(Page 9)*
9:45	Ticia Buhr	Azimuth angle dependence of the He 1s and Ne 2s photoelectron angular distributions *(Page 10)*
10:10		Coffee break
10:40	Paola Bolognesi	Radiation damage in systems of biological interest: the case of radiosensitisers *(Page 11)*
11:25	Alexei Grum-Grzhimailo	Coherent control of electron emission in short-pulse XUV atomic ionization *(Page 12)*
11:50	Andrej Bunjac	Calculation of the dynamic Stark shift for sodium and the application to resonantly enhanced multiphoton ionization *(Page 13)*
12:15		Lunch

Electron and photon interactions - *Chairman*: Martin Čížek

14:00	Petr Dohnal	Laboratory study of electron-ion recombination and of associative detachment at low temperatures *(Page 14)*
14:25	Roman Čurík	Inelastic low-energy collisions of electrons with small cations *(Page 15)*
14:50	Petra Votavová	Superexchange Interatomic Coulombic decay by Fano-ADC-Stieltjes method *(Page 16)*
15:15	Viorica Stancalie	Studies of the electron-correlation and relativistic effects in target representation and low-energy collision calculations *(Page 17)*
15:40		Coffee break
16:15		Poster Session, International Scientific Committee meeting
19:00		Individual dinner

Tuesday, September 5

Ion interactions - *Chairman*: Robert DuBois

9:00	Alicja Domaracka	Ion collisions with complex molecular systems: isolated molecules, clusters and astrophysical ices *(Page 18)*
9:45	Sándor Kovács	Dissociative ionization of H_2O molecule bombarded by single charged projectiles *(Page 19)*
10:10		Coffee break
10:40	Jeff Shinpaugh	Experimental and computational study of gold nanoparticles as a radiosensitizer for proton radiation *(Page 20)*
11:25	François Frémont	Classical treatment of autoionization in slow ion-atom collisions *(Page 21)*
11:50	Nikolaus Stolterfoht	Milestones of highly charged ion guiding through insulating cappillaries: applications to a conical sphape *(Page 22)*
12:15		Lunch
14:20		Departure to Prague, Excursion
19:00		Conference Dinner in the Strahov Monastery Brewery

Wednesday, September 6

Electron-impact experiments - *Chairman*: Gustavo García

9:00	Janina Kopyra	Low energy electron driven decomposition of biologically relevant molecules *(Page 23)*
9:45	Marián Danko	Dissociative ionization of cyclopropylamine *(Page 24)*
10:10		Coffee break
10:40	Paulo Limão-Vieira	Decomposition of nitroimidazoles by electron impact *(Page 25)*
11:25	Jaroslav Kočišek	Does pinene stabilize water aerosols? *(Page 26)*
11:50	Nigel Mason	Electron driven chemistry on comet 67P observed by Rosetta space craft and its implications *(Page 27)*
12:15		Lunch
14:00		Departures or individiual afternoon in Prague

List of Posters

Abstracts of Oral Contributions

Attochemistry: imaging and controlling electron dynamics in molecules

F. Martín[1,2,3]

[1]*Departamento de Química, Módulo 13, Universidad Autónoma de Madrid, 28049 Madrid, Spain*

[2]*Instituto Madrileño de Estudios Avanzados en Nanociencia (IMDEA Nano), Campus de Cantoblanco, 28049 Madrid, Spain*

[3]*Condensed Matter Physics Center (IFIMAC), Universidad Autónoma de Madrid, 28049 Madrid, Spain*

Attosecond light pulses allow one to probe the inner workings of atoms, molecules and surfaces on the timescale of the electronic motion. For example, in molecules, sudden ionization by an attosecond pulse is followed by charge redistribution on a time scale from a few-femtoseconds down to hundreds attoseconds, which is usually followed by fragmentation of the remaining molecular cation. Such complex dynamics arises from the coherent superposition of electronic states covered by the broadband attosecond pulse and from rearrangements in the electronic structure of the molecular cation due to electron correlation. To investigate these ultrafast processes, attosecond pump-probe and transient absorption spectroscopies have been shown to be very valuable tools [1–3]. In this talk I will present the results of molecular attosecond pump-probe experiments and theoretical simulations in which several molecules, from the simplest H_2 one to the aminoacids phenylalanine and tryptophan, are ionized with a single attosecond pulse (or a train of attosecond pulses) and are subsequently probed by one or several infrared or xuv few-cycle pulses. In all cases, the evolution of the electronic and nuclear densities in the photo-excited molecule or remaining molecular ions can be inferred from the measured (or calculated) ionization or fragmentation yields with attosecond time-resolution, and can be visualized by varying the delay between the pump and probe pulses. The results of these pioneering works will certainly serve as a guide of future experimental efforts in more complicated molecules and may open the door to the control of charge transfer in biologically relevant processes [3].

[1] G. Sansone *et al.*, Nature **465** (2010) 763.
[2] F. Calegari *et al.*, Science **346**, (2014) 336.
[3] M. Nisoli, *et al.*, Chem. Rev. DOI: 10.1021/acs.chemrev.6b00453.

Azimuth angle dependence of the He 1s and Ne 2s photoelectron angular distributions

T. Buhr[1,2], L. Ábrók[2], Á. Kövér[2], B. Pollakowski-Herrmann[3], J. Weser[3], J. Dreismann[1], D. Nagy[2], D. Paul[1], D. Varga[2], A. Müller[4], B. Beckhoff[3], S. Schippers[1], S. Ricz[2]

[1]*I. Physikalisches Institut, Justus-Liebig-Universität Gießen, 35392 Gießen, Germany*

[2]*Institute for Nuclear Research, Hungarian Academy of Sciences, 4001 Debrecen, Hungary*

[3]*Physikalisch-Technische Bundesanstalt (PTB), 10587 Berlin, Germany*

[4]*Institut für Atom- und Molekülphysik, Justus-Liebig-Universität Gießen, 35392 Gießen, Germany*

Higher-order multipoles strongly modify the polar and azimuth angle dependences of the differential photoionization cross sections [1]. In order to study the azimuth angle dependence, 3D photoelectron angular distributions must be experimentally determined. 3D angular distributions of photoelectrons of the He 1s and Ne 2s shells were measured as a function of the polar and azimuth angles at photon energies 100 eV and 200 eV employing linearly polarized synchrotron radiation. The experiments were carried out at the beam line PTB-XRS on the third generation storage ring BESSY II at HZB (Berlin, Germany). The emitted electrons were analyzed using an ESA-22-type electrostatic electron spectrometer developed at Atomki (Debrecen, Hungary) [2,3]. The photoelectrons were detected in the polar angular range (χ) of $\pm 15°$ to $\pm 165°$ in $15°$ steps relative to the photon momentum vector ($\mathbf{k}$) and in the azimuth angular range (χ) of $0°$ to $90°$ as well as $180°$ to $270°$ in $15°$ steps (see Fig. 1.a). Figure 1.b shows the experimental 3D angular distribution of photoelectrons of the He 1s shell at photon energy 100 eV. As far as we know, these are the first experiments where 3D photoelectron angular distributions were observed.

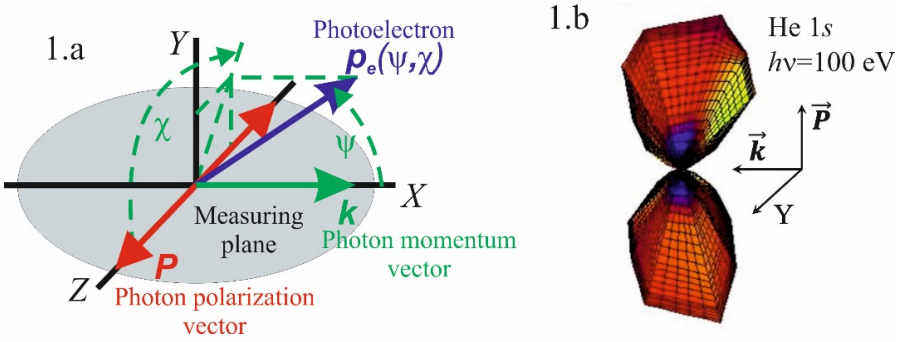

Figure 1: 1.a: Measuring geometry; 1.b: Experimental 3D angular distribution of the He 1s photoelectrons at photon energy 100 eV

The assistance of the staff of the beam line PTB-XRS is gratefully acknowledged. This work was supported by the Hungarian Scientific Research Foundation (OTKA, Grant No.: K104409) as well as by the German Federal State of Hessen through the LOEWE funding scheme (project ELCH).

[1] A. Derevianko *et al.*, At. Data Nucl. Data Tables **73** (1999) 153.
[2] S. Ricz *et al.*, Phys. Rev. A **65** (2002) 042707.
[3] L. Ábrók *et al.*, Nucl. Instrum. Methods B **369** (2016) 24.

Radiation damage in systems of biological interest: the case of radiosensitisers

Paola Bolognesi
CNR-ISM, Area della Ricerca di Roma 1, Monterotondo Scalo (Roma), Italy

In the past decades, major improvements have been achieved in cancer treatment by combining radio- and chemo-therapy. In these treatments drugs specifically designed to selectively enhance the effectiveness of different radiation sources on tumor rather than healthy cells are supplied to the patients. Halo-substituted DNA bases [1-3] and nitroimidazoles [1,4] are two classes of radiosensitisers, and their mechanisms of functioning are very different. While the first act on the DNA of the tumor cells, the second is very effective against hypoxic tumors as oxygen mimetic species.

Tunable synchrotron radiation at Elettra (Trieste) has been used to perform mass spectrometry, electron photoemission and electron-ion coincidence (PEPICO) experiments on both valence and inner-valence orbitals of several representatives of these two different classes of radiosensitisers. In this presentation several examples will be given to show that electron and ion spectroscopic studies, coincidence experiments and theoretical calculations of isolated biomolecules in the gas phase not only are feasible, but provided detailed spectroscopic characterisation of relatively complex biomolecular species, providing deep insight into the peculiar mechanism that might differentiate their specific functioning as radiosensitisers.

Figure 1 shows the example of 2Br-pyrimidine, a halo-substituted DNA base, where the results of PEPICO experiments performed at several kinetic energies of the photoelectron (top), reported versus binding energy (middle), display a clear state-selectivity in the molecular fragmentation of this molecule. This can be related to the peculiar charge distribution of individual molecular orbitals, (bottom). For the parent ion, the first three orbitals are characterized by large Mulliken population on the Br atom and are antibonding. Thus the ionisation of these orbitals reinforces the C–Br bond and the molecule does not fragment. In the $n_{\perp}$ orbital the lone pair of the halogen atom is a bonding orbital. The ionization process involving this orbital weakens the C–Br bond leading to the loss of Br-radical, a very reactive species. On the contrary, the HCN loss corresponds to the binding energy region of the π_1 orbital that, being delocalized above and below the ring, once ionized may favour the ring breaking at the N3–C2 and C4–C5 bonds. Specific consequences may arise in the two cases.

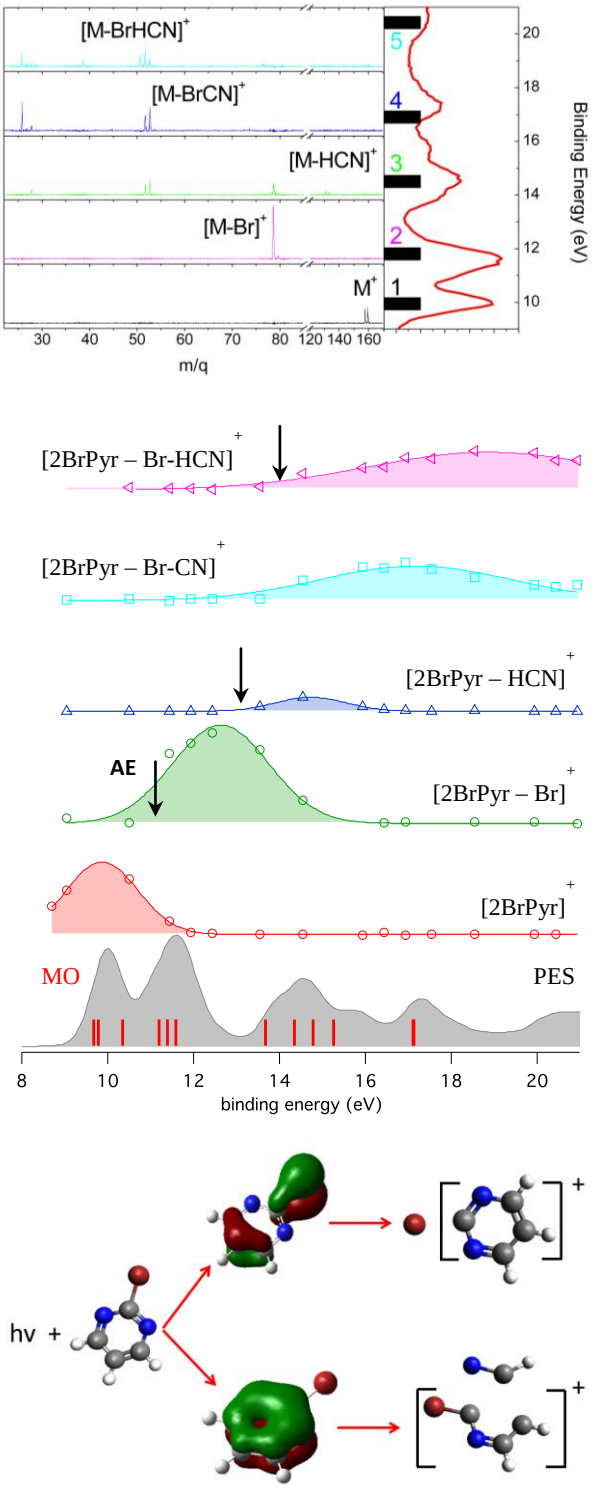

Figure 1. The 2Br-pyrimidine molecule photoelectron-photoion coincidence (PEPICO) measurement showing state-selective fragmentation.

References

[1] M. Poggi et al. Current Problems in Cancer 25 (2001) 331.
[2] M.C. Castrovilli et al. J. Am. Soc. Mass Spectrom. 25 (2014) 351-367.
[3] P. Bolognesi et al. Phys. Chem. Chem. Phys. 17 (2015) 24063-24069
[4] P. Bolognesi et al. J.Chem. Phys. 145 (2016) 191102.

*E-mail: paola.bolognesi@cnr.it

Coherent control of electron emission in short-pulse XUV atomic ionization

A.N. Grum-Grzhimailo[1]

[1]*Skobeltsyn Institute of Nuclear Physics, Lomonosov Moscow State University, Leninskie gory 1, 119991, Moscow, Russian Federation*

In a coherent control scheme, a quantum system is driven from an initial to a specific final state via different pathways with corresponding interfering transition amplitudes. Control of the outcome of the reaction is achieved by changing the phase between the amplitudes. In atomic ionization, coherent control is generally accomplished by using coherent light sources. Varying the phase between the electromagnetic waves, for example, between two different harmonics, leads to the control of the photoemission flux. Up to recently such processes were available only in the optical range (see, for example, the review [1] and references therein) and even used to extract relative amplitudes for photoionization into channels with different parity. In 2016 such a scheme was realized with femtosecond VUV pulses from free-electron laser (FEL) FERMI (Trieste, Italy) [2], thereby opening a new avenue in nonlinear optics in the XUV frequency regime.

The talk concentrates on a few examples of controlling the angular distribution of the photoemission generated by intense bichromatic XUV radiation, consisting of the fundamental (nonlinear second-order ionization process) and its second harmonic (linear ionization process). The interference of the two ionization paths manifests itself through a counterintuitive symmetry violation in the angular distribution of the photo-emission: for linearly polarized radiation the symmetry with respect to the plane perpendicular to the polarization vector is broken, while for circularly polarized light the axial symmetry with respect to the photon beam is violated. The degree of this asymmetry depends on the strength of the fundamental and the harmonics. It shows an oscillatory behavior as function of the relative phase of the harmonics and, in certain cases, can provide important information regarding the phases of the harmonics generated by FELs. Specific effects on the asymmetry are predicted for the case when the fundamental scans an intermediate resonance, i.e. one of the ionization paths is a two-photon resonant transition. In the resonance region, an analytic parameterization of the asymmetry can be derived as function of the photon energy within the lowest nonvanishing order of perturbation theory.

Selected illustrative examples will include hydrogen and neon atoms with calculations performed in perturbation theory as well as by solving the time-dependent Schödinger equation [3–5].

The author would like to acknowledge K. Bartschat, N. Douguet, E.V. Gryzlova, E.I. Staroselskaya, G. Sansone, K. Prince, and K. Ueda for collaboration and fruitful discussions.

[1] V.A. Astapenko, Quantum Electron. **36** (2006) 1131.
[2] K. C. Prince *et al.*, Nat. Photonics. **10** (2016) 176.
[3] A.N. Grum-Grzhimailo *et al.*, Phys. Rev. A **91** (2015) 063418.
[4] N. Douguet*et al.*, Phys. Rev. A **93** (2016) 033402.
[5] N. Douquet *et al.*, Eur. Phys. J. D **71** (2017) 105.

Calculation of the dynamic Stark shift for sodium and the application to resonantly enhanced multiphoton ionization

A. Bunjac[1], D. B. Popović[1], N. S. Simonović[1]

[1]*Institute of Physics, University of Belgrade, P.O. Box 57, 11001 Belgrade, Serbia*

Although several monographs on the topic of the resonant dynamic Stark shift (RDSS) have been published [1,2], accurate data in a wage range of parameters is still not available for most systems studied. A method for determining the RDSS, based on wave-packet calculations of the population probabilities of quantum states, is presented. It is almost insensitive to variations of the laser pulse profile, which ensures a generality in applications. The method is used to determine an RDSS data set for transitions $3s \rightarrow nl$ ($n \leq 6$) in sodium induced by the laser pulse with the peak intensities up to $7.9 \times 10^{12}\,\mathrm{W/cm^2}$ and wavelengths in the range from 455.6 to 1139 nm. The data is applied to analyze the photoelectron spectra (electron yield versus excess energy) of the sodium atom interacting with an 800 nm laser radiation. Substructures observed in the recent experimentally measured spectra [3] are successfully reproduced and related to the resonantly enhanced multiphoton ionization (REMPI) via specific (P and F) intermediate states.

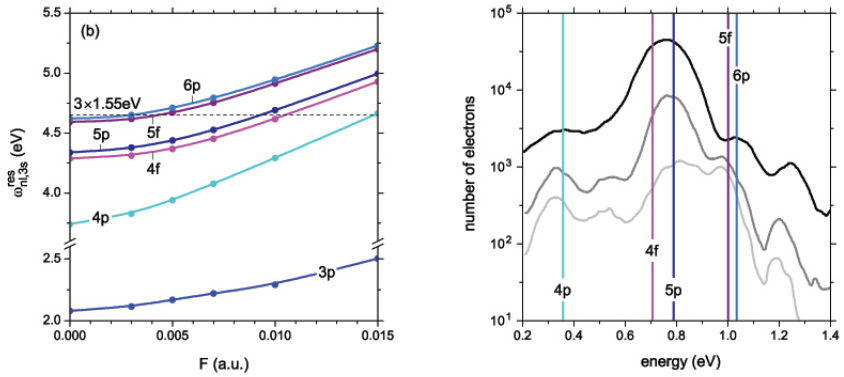

Figure 1: Left: The field-strength dependence of excited states energies relative to the ground state energy for the sodium atom in the laser field which is in K-photon resonance with transitions $3s \rightarrow nl$ K = 1 and K = 3. Horizontal dashed line marks the three-photon energy, for the laser field of 800 nm wave length. Right: Calculated values for photoelectron excess energies (vertical lines) which characterize four-photon REMPI of sodium via 4p, 4f, 5p, 5f and 6p states by 800nm laser field, shown together with experimentally measured electron yield versus photoelectron excess energies obtained for 57 fs laser pulse with peak intensities $3.5 \times 10^{12}\,\mathrm{W/cm^2}$ (white gray, lower curve), $4.9 \times 10^{12}\,\mathrm{W/cm^2}$ (gray, middle curve), and $8.8 \times 10^{12}\,\mathrm{W/cm^2}$ (black, upper curve) [3].

[1] N. B. Delone and V. P. Krainov, Multiphoton Processes in Atoms, Vol. 13, Springer, Heidelberg, 2000.
[2] M. Fox, Quantum Optics: An Introduction, Oxford University Press, New York, 2006. p. 167.
[3] N. A. Hart *et al.*, Phys. Rev. A **93** (2016) 063426.

Laboratory study of electron-ion recombination and of associative detachment at low temperatures

P. Dohnal[1], Á. Kálosi[1], D. Shapko[1], R. Plašil[1], A. Kovalenko[1], T.D. Tran[1], S. Rednyk[1], Š. Roučka[1], J. Glosík[1]

[1]*Department of Surface and Plasma Science, Faculty of Mathematics and Physics, Charles University, V Holešovičkách 2, 180 00 Prague, Czech Republic*

The results of experimental studies of elementary processes relevant for description of low temperature hydrogen/deuterium containing plasma are reported. The studies include electron ion recombination and associative detachment processes. Stationary afterglow experiment with cavity ring down absorption spectrometer (SA-CRDS) was used to study the electron-ion recombination of H_3^+, H_2D^+, HD_2^+, D_3^+ and N_2H^+ ions in low temperature (77-350 K) plasmas in He buffer gas with small fraction of ion forming gases (H_2, D_2, N_2) (for details see e.g. [1–3]). In the experiments the number densities, kinetic and rotational temperatures of recombining ions during the afterglow were monitored using time resolved cw-CRDS spectroscopy. To obtain the binary and eventual ternary recombination rate coefficients for particular ions, dependencies of overall recombination rate coefficient (effective rate coefficient for particular composition of mixture of ions) on He pressure and on partial pressures of ion forming gases were measured. Formation of H_2O (and D_2O) via associative detachment in reaction of O^- anion with H_2 (and D_2) was studied at temperatures from 10 K up to 300 K using cryogenic 22-pole ion trap (for further experimental details see [4, 5] and references therein). The temperature dependencies of the reaction rate coefficients for the two exothermic reaction channels (associative detachment and atom transfer) for both reactants were determined. Particular attention was paid to isotope effect.

This work was partly supported by the Czech Science Foundation (GACR 15-15077S, GACR 17-08803S, GACR 17-19459S, GACR 17-18067S) and by the Charles University (project Nr. GAUK 1583517, GAUK 1144616, GAUK 1168216).

[1] P. Dohnal *et al.*, J. Chem. Phys. **136** (2012) 244304.
[2] P. Rubovič *et al.*, J. Phys. Chem. A **117** (2013) 9626.
[3] R. Plašil *et al.*, Plasma Sources Sci. Technol. **26** (2017) 035006.
[4] P. Jusko *et al.*, Int. J. Mass Spectrom. **352** (2013) 19.
[5] P. Jusko *et al.*, J. Chem. Phys. **142** (2015) 014304.

Inelastic low-energy collisions of electrons with small catios

R. Čurík[1], C.H. Greene[2]

[1] *J. Heyrovský Institute of Physical Chemistry, Academy of Sciences of the Czech Republic, v.v.i., Dolejškova 3, 182 23 Prague 8, Czech Republic*
[2] *Department of Physics and Astronomy, Purdue University, West Lafayette, Indiana 47907, USA*

We present a detailed study of inelastic low-energy (0–1 eV) collisions of electrons with HeH^+ cations. Our results include rovibrational excitation and dissociative recombination (DR) channels:

$$\begin{aligned} HeH^+(\nu, j) + e^- &\rightarrow HeH^+(\nu', j') + e^- \\ HeH^+(\nu, j) + e^- &\rightarrow He + H \end{aligned}$$

We apply *ab initio* multichannel quantum defect theory (MQDT) according to which both studied processes are described by the Born-Oppenheimer quantum defects. The quantum defects were determined using the R-matrix approach. We obtain good agreement with the available theoretical prediction of the rotationally inelastic thermal rates. Our computed DR rate is also in very good agreement with available experimental results. Moreover, several computational experiments allowed us to study a role of rotational and vibrational excitations in the indirect DR mechanism governing the HeH^+ dissociation. While the rotational excitation is several orders of magnitude more probable process at the studied collision energies, the closed-channel resonances described by the high-n, rotationally excited neutral molecules of HeH, contribute very little to the dissociation probability. Situation is very different for resonances defined by the high-n, vibrationally excited HeH molecules. These are found to dissociate with about 90% probability [1].

[1] R. Čurík and C. H. Greene, J. Chem. Phys **147** (2017) 054307.

Superexchange Interatomic Coulombic decay by Fano-ADC-Stieltjes method

P. Votavová[1], T. Miteva[2], S. Kazandjian[2], P. Kolorenč[1], N. Sisourat[2]

[1]*Institute of Theoretical Physics, Faculty of Mathematics and Physics, Charles University, V Holešovičkách 2, 180 00 Praha 8, Czech Republic*

[2]*Laboratoire de Chimie Physique Matière et Rayonnement, Sorbonne Universités, UPMC Univ Paris 06, UMR 7614, F-75005 Paris, France*

Fano-ADC-Stieltjes is an *ab initio* $\mathcal{L}^2$ method for the calculation of the decay width of metastable states of atoms, molecules and their clusters. It relies on Fano-Feshbach theory of resonances to describe the metastable state as a discrete state embedded in a continuum of final states. Algebraic diagrammatic construction in intermediate states representation (ISR-ADC) is used to construct many-electron wave functions. Correct renormalization of discretized continuum is achieved by Stieltjes imaging technique. Favorable numerical properties are fast convergence and size extensivity. We assess this method as the most efficient one for studying non-radiative relaxation processes such as Auger effect or Interatomic Coulombic decay (ICD). In ICD, an inner-valence vacancy is filled by an outer-valence electron and the excess energy is transferred to a neighboring atom which is thus ionized. We study new ICD mechanism called superexchange ICD in NeHeNe trimer. We demonstrate that the decay width of Ne dimer increases significantly in the presence of the bridge He atom. The enhancement is due to the electron transfer between the Ne atom and virtual states of the ICD-inactive He, driven by inter-atomic electron correlation.

Studies on the electron-correlation and relativistic effects in target representation and low-energy collision calculation

V. Stancalie[1]

[1]*National Institute for Laser, Plasma and Radiation Physics, Atomistilor 409, P.O.Box MG-36, Magurele-Ilfov, 077125 Romania*

This work is motivated by a long standing discrepancy between the theoretical models treating the complexity of the resonance structure for low-energy electron scattering. This complexity of the resonance structure for low-energy electron scattering determines the complexity of atomic data calculation. In this respect, current theoretical method and computational tools place more emphasis on the accurate representation of target electron wave functions than the study of other processes. The cross section and rates must be determined at typically tens of thousands of energy values. As the charge number Z on the atomic nucleus increases, relativistic effects become progressively more important in the collision process. In this work we consider how these effects can be accurately represented in low-energy electron collisions with heavy atoms and atomic ions. We have systematically investigated whether the differences in the calculations of atomic data for the Mg-like S V, S-like Ar III, Li-like Al XI ions and the Fe-peak element Co IV ion, are due to the different treatment of relativistic effects or to the approximation made in solving the resultant scattering equations. We have carried out calculations using several procedures for including electron correlation and relativistic effects, ranging from transforming the non-relativistic K-matrix to solving the Dirac equation in case of the Mg-like S V ion [1, 2]. An important question is where can accurate results be obtained using the Breit-Pauli Hamiltonian, and when is it necessary to use the Dirac Hamiltonian. We have addressed this important issue for the S-like Ar III ion [3] and for the Fe-peak element Co IV ion [4, 5]. It has been realized that transitions from autoionizing levels (so-called dielectronic satellites) of highly charged ions provide an outstanding plasma temperature diagnostic. We have performed detailed quantitative description of the level population kinetics responsible for the relatively high line-intensity of the forbidden and intercombination transitions arising from autoionizing states in Li-like Al [6]. Anomalous high intensity X-ray intercombination and two-electron transitions in verifying the conditions stated here have been detected at the nhelix-laser test bed facility at GSI.

[1] V. Stancalie *et al.*, Atomic Data for transitions in SV, Paper presented at the 19th International Conference on Atomic Processes in Plasmas, 4-8 April 2016, Paris.
[2] C Iorga and V. Stancalie, At. Data Nucl. Data Tables (2016) doi: 10.1016/j.adt.2016.06.002.
[3] V. Stancalie *et al.*, Eur. Phys. J. D **66** (2012) 84.
[4] V. Stancalie, Phys. Scr. **83** (2011) 025301; J. Spectroscopy (2013) 820635.
[5] K. M. Aggarwal *et al.*, At. Data Nucl. Data Tables **107** (2016) 140.
[6] C. Iorga and V. Stancalie, Can. J. Phys. **93** (2015) 1413.

Ion collisions with complex molecular systems: isolated molecules, clusters and astrophysical ices

A. Domaracka[1]

[1]*Normandie Univ, ENSICAEN, UNICAEN, CEA, CNRS, CIMAP, 14000 Caen, France*

Carbon containing molecules are ubiquitous in our Universe. The sizes of carbonaceous systems cover a very large range: from small molecules (hydrocarbons), via large complex molecular systems (e.g. fullerenes and polycyclic aromatic hydrocarbons – PAHs, heterocyclic molecules...) and its clusters up to micrometer-sized grain particles. On the one hand, the formation pathway of carbonaceous matter in astrophysical environments, as well as in planetary atmospheres is not fully understood. On the other hand, the studies on survival of heterocyclic molecules (like nucleobases) in astrophysical environments are required.

In the first part of the talk, I will give an overview of recent results on ion-induced molecular growth processes of carbon containing clusters (e.g. pyrene, butadiene) colliding with slow ions (Fig.1). Molecular growth is driven by the prompt fragmentation of molecules in loosely bound clusters when the impacting projectile ion deposits a large amount of energy and momentum to individual atoms through nuclear scattering (knock-out processes) leading to formation of reactive species. These molecular fragments may form covalent bonds with neighboring molecules in the cluster on sub-picosecond time scales, well before the excited cluster dissociates [1]. In the second part of the talk, I will present recent studies on the radiolysis of nucleobases in the solid phase at low temperature induced by swift heavy ion beams, which allow to simulate in the laboratory cosmic ray irradiation of such molecules in space. We have estimated half-life-time of such molecules in dense clouds based on the found relation between the destruction cross sections (σ_d) and the electronic stopping power ($\sigma_d \; S_e^n$, where n $1.2 - 1.3$ for adenine [2] and cytosine molecules, respectively).

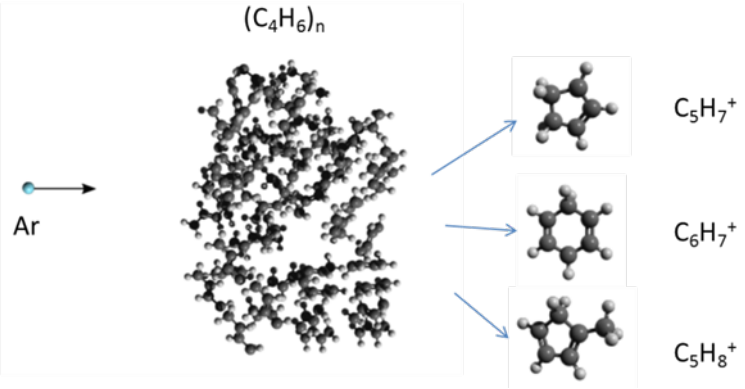

Figure 1: An example of an Ar atom which collides with a randomly oriented $[C_4H_6]_{50}$ cluster and selected cyclic growth products.

[1] M. Gatchell *et al.*, PCCP (2017) in print; R. Delaunay *et al.*, J. Phys. Chem. Lett. **6** (2015) 1536; H. Zettergren *et al.*, Phys. Rev. Lett. **110** (2013) 185501.

[2] G.S. Vignoli Muniz *et al.*, Astrobiology **17** (2017) 298.

Dissociative ionization of H_2O molecule bombarded by single charged projectiles

S.T.S. Kovács[1], P. Herczku[1], Z. Juhász[1], L. Sarkadi[1], L. Gulyás[1], B. Sulik[1]

[1]*Institute for Nuclear Research, Hungarian Academy of Science (ATOMKI), Bem tér 18/c, 4026 Debrecen, Hungary*

We report measurements on fragmentation cross sections of water. From the yields of the fragments we deduced the multiple ionization cross sections, and compared them with the results of theoretical predictions.

Dissociation of the gas phase water molecule was measured by 1 MeV H^+, He^+ and 650 keV N^+ impact in crossed beam experiments. The energy and angular distribution of the charged fragments were analyzed by a rotatable, energy-dispersive electrostatic spectrometer. Absolute double-differential fragmentation cross sections were determined.

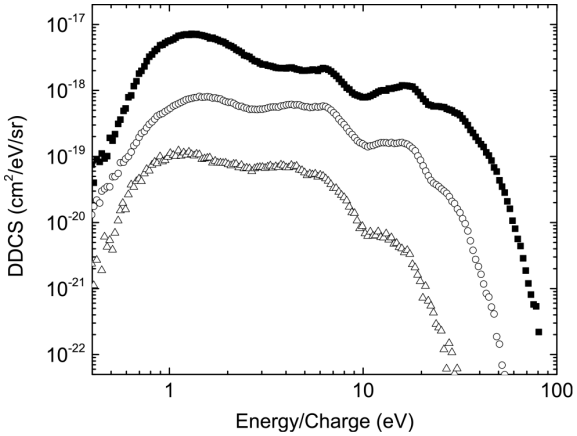

Figure 1: Double-differential fragmentation cross sections for the H_2O molecule. Open triangles stands for H^+ impact, open circles for He^+ and full squares for N^+ projectile.

The total cross section is increasing more than two orders of magnitude from H^+ to N^+ as it is shown in Figure 1. Two different regions of the fragment ions can be identified: The large peak below 3 eV contains dominantly heavy fragments (OH^+; O^{q+}). The structured region above 3 eV is due to H^+ fragments from the different fragmentation channels. The energy of the H^+ ions is increasing towards higher ionization degrees of the H_2O^{q+} transient molecular ion (due to Coulomb explosion) [1]. Therefore H^+ fragments from the double, triple, four-fold or five-fold ionized H_2O^{q+} molecules appear in the energy ranges of 4-15 eV, 16-28 eV, 30-40 eV and >45 eV respectively [2]. The maximal ionization degrees were $q_{\max} = 3$, 4, and 5 for H^+, He^+ and N^+ impact respectively. These increasing target charge states are attributed to the decreasing impact velocities, and increasing effective charges, i.e., the increasing average perturbation strength from H^+ to N^+ [3].

For the quantitative analysis, the spectra were fitted with Gaussians based on the available KER data in the literature. From the fits we deduced the multiple ionization cross sections, and compared them with the results of the quantum mechanical CDW-EIS and the classical CTMC calculations. With increasing degree of ionization the theoretical multiple ionization cross sections more and more overestimate the experimental data. It is attributed to the incompleteness of the independent particle model (IPM), namely that it cannot account for electron correlation. Additionally, we found that the relative importance of the electron correlation depends on the ratio of the average value of the correlation energy to that of the energy transfer, which is characteristic for the collision.

Work was supported by the Hungarian National Science Foundation (OTKA, K109440).

[1] J. Rajput *et al.*, Phys. Rev. A **84** (2011) 052704.
[2] H. Luna *et al.*, J. Phys. B. **36** (2003) 4717.
[3] S.T.S. Kovács *et al.*, Phys. Rev. A **94** (2016) 012704.

Experimental and computational study of gold nanoparticles as a radiosensitizer for proton radiation

J.L. Shinpaugh[1], E.C. Maertz[1], W.L. Hawkins[1], T.M. Mendenhall[1], N. Carlson[1], C. Boyd[1], J. Teller[1], C. Putnam-Evans[2], R.A. McLawhorn[3], L.H. Toburen[1], M. Dingfelder[1]

[1]*Department of Physics, East Carolina University, Greenville, North Carolina, 27858 USA*

[2]*Department of Biology, East Carolina University, Greenville, North Carolina, 27858 USA*

[3]*21st Century Oncology, Greenville, North Carolina, 27834 USA*

The use of nanoparticles as radiosensitizers is widely being studied for enhancing tumor cell killing in radiation therapy for the treatment of cancer. At East Carolina University, we have initiated an experimental and computational study of gold nanoparticles as a radiosensitizer for particle radiation. Results are presented for cell survival and radiation damage for in-vitro irradiation by protons of malignant prostate and breast epithelial cells treated with gold nanoparticles in an energy range approaching the Bragg peak (maximum stopping power near the end of the particle track). These results are intended to serve as benchmark data as interest expands for using a wide range of materials as radiosensitizers in hadron therapy; comparison to our previous results for proton irradiation of nonmalignant and cancer cells treated with cerium oxide nanoparticles will be presented.

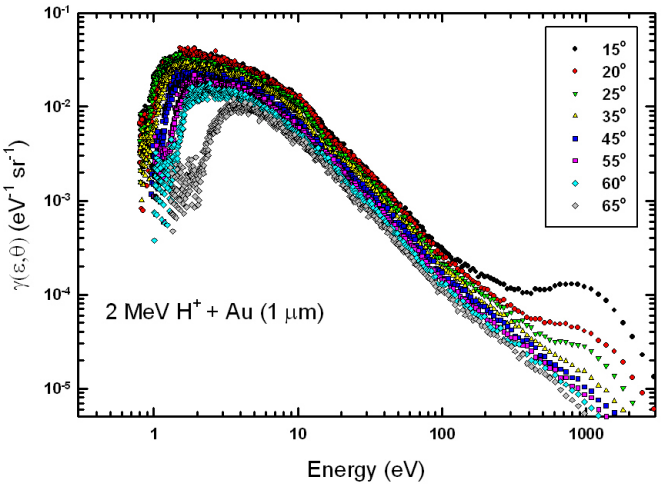

Figure 1: Absolute doubly differential electron emission yields for 2-MeV protons incident on a 1-μm gold foil. Spectra are shown for various emission angles relative to the incident beam.

In addition, we are expanding current Monte Carlo track structure simulation models to include secondary electron production from gold. To test the models, we have measured absolute doubly differential electron emission yields from gold surfaces and hydrated gold surfaces induced by fast proton impact. Typical electron emission spectra are shown in figure 1 for electron emission in the forward direction with respect to the incident proton beam. Current results will be compared to previous experimental and simulated results for proton-induced electron transport in water [1].

[1] L.H. Toburen *et al.*, Radiation Research **174** (2010) 107.

Classical treatment of autoionization in slow ion-atom collisions

F. Frémont[1]

[1]*Université de Caen-Normandie, CIMAP, 6 bd du Mal Juin 14050 Caen Cedex France*

While many experiments have been devoted to double capture (DC) in slow ion-atom collisions, theory still remains a challenge, since electron-electron correlation, which cannot be neglected, especially at very low energies, is difficult to take into account. We present here a classical model to treat theoretically DC process in 150 keV Ne^{10+} + He collisions [1]. Since configurations 3lnl' and 4lnl' are mainly populated, autoionization takes a large place during the collision. CTMC model is used to calculate DC cross sections, and to separate autoionizing DC (ADC) and non autoionizing DC (NADC). The problem to solve is a true four-body problem, including electron-electron interaction. In addition to Coulombic potentials, phenomenological potentials are introduced to insure the stability of He target [2].

Figure 1 shows typical integration time evolution of single ionization (SI) and ADC cross sections ($t = 0$ corresponds to time for which Ne^{10+} and He are in a plane perpendicular to the incident projectile direction).

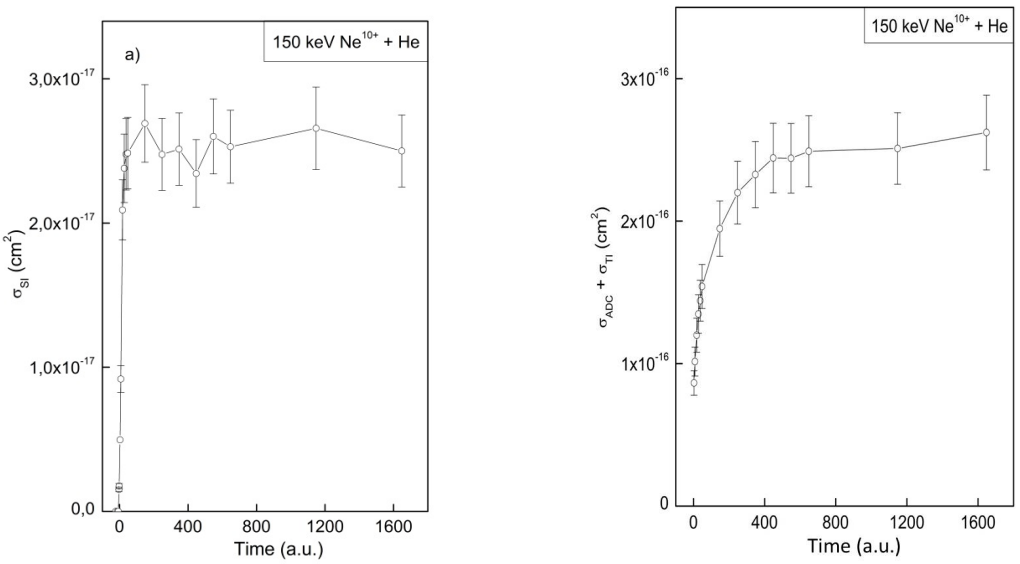

Figure 1:

For SI (left side), cross section remains constant just after the collision, i.e. after about 50 a.u. of integration time. In contrast, ADC cross section slowly increases exponentially from 0 to 800 a.u., indicating that the projectile may deexcite via autoionization. A fit using an exponential function shows that the average autoionization width is of the order of 200 a.u., and is of the same order of magnitude than that found experimentally. Note that Transfer-Ionization (TI) leads to the same final states than for ADC. However, at low projectile energies, TI is expected to be negligible. In conclusion, the present work clearly proves that a typical quantum effect can be classically treated. This will be used in the future in many multi-body collisions.

[1] F. Frémont, to be published.
[2] J.S. Cohen, Phys. Rev. A **51** (1995) 266.

Milestones of highly charged ion guiding through insulating capillaries: Applications to a conical shape

N. Stolterfoht[1]

[1]*Helmholtz-Zentrum Berlin für Materialien und Energie, 14109 Berlin, Germany*

After the first observation that keV ions are guided through insulating nanocapillaries [1], the topic has received considerable attention during the last decade. With increasing charge deposition by the indecent ions, a charge patch is formed until the electrostatic field is large enough to deflect the ions. The essential property of the capillary guiding is a self-organizing charge deposition, which governs the ion passage through the capillary. At equilibrium, the ions are guided maintaining their incident charge state [1,2].

Milestones of the field are discussed in accordance with a recent review concerning the extensive studies of capillary guiding [3]. Recent experiments with insulating nano- and micro-capillaries are presented. Similarities as well as significant differences between the capillary types are pointed out. Apart from the experimental studies, theoretical concepts of the capillary guiding are presented. Single tapered capillaries are discussed involving an enhancement of the beam density and the production of a microbeam for various applications including biological matter. Fig. 1 shows results of calculations using a drift

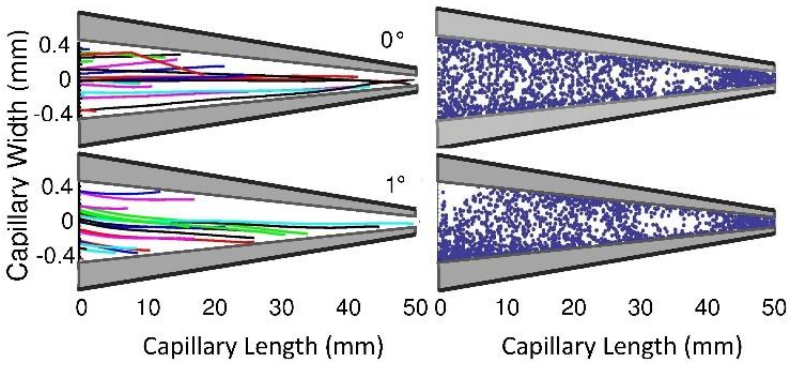

Figure 1: Calculations of 4.5-keV Ar^{7+} ions incident at 0° and 1° into a conical capillary [4].

model for trajectories and charge distributions for 4.5-keV Ar^{7+} incident under 0° and 1° into a conical microcapillary [4,5]. The simulations show that the density of the transmitted ions is enhanced by a factor more than 4. In addition, the theoretical results confirm an unexpected experimental observation of a minimum in the emission profiles at zero observation angle. Altogether, it is shown that capillary guiding involves several novel phenomena whose understanding has made essential progress.

[1] N. Stolterfoht *et al.*, Phys. Rev. Lett. **88** (2002) 133201.
[2] K. Schiessl *et al.*, Phys. Rev. A **72**(2005) 062902.
[3] N. Stolterfoht and Y. Yamazaki, J. Phys Rep. **629** (2016) 1.
[4] N. Stolterfoht *et al.*, Phys. Rev. A **91** (2015) 32709.
[5] N. Gruber *et al.*, Nucl. Instr. Methods B **314** (2014) 1.

Low energy electron driven decomposition of biologically relevant molecules

J. Kopyra[1]

[1]*Siedlce University, Faculty of Science, 3 Maja 54, 08-110 Siedlce, Poland*

Electron impact processes with molecules play a crucial role in a wide range of phenomena and have been the subject of considerable research interest since mid of the last century. An understanding of these processes is important in various fields of applied physics including radiation physics and chemistry [1].

Nearly twenty years ago it has been shown that low energy electrons (LEEs) have the propensity to severely damage biomolecules including vital DNA macromolecule. This became obvious from the landmark experiment performed by the group of L. Sanche [2] in which it has been shown that LEEs can effectively cause strand breaks already at energies below the ionization threshold of DNA. A particular importance of this observation stems from the fact that the deposition of energy by primary high energy quanta in the biological medium generates secondary electrons as the most abundant secondary products [3]. As a matter of fact, the yield of these secondary species is about 5×10^4 per MeV of deposited radiation energy and essentially comprise electrons with kinetic energies < 20 eV [4, 5]. Hence, reactions induced by the low energy electrons are considered as important and decisive steps in the description of radiation damage to biological systems [6, 7]. In this contribution, the dissociative electron attachment (DEA) to chemical agents frequently used in chemotherapy will be discussed. It appears, that some of these drugs have a propensity to specifically and selectively sensitize cancer cells [8] during their synchronous administration with the ionizing radiation. Such compounds can be represented by the so-called antimetabolites which exhibit high structural similarity to the naturally occurring metabolites. Therefore, they readily become incorporated into DNA and hence interfere with the cells normal metabolic functioning. This group includes, e.g., halogenated nucleobases as well as sulphur containing analogue of canonical nucleobases [9, 10]. During this talk the main outcomes from DEA to sulphur containing nucleobases will be presented and discussed.

[1] L.G. Christophorou, Electron Molecule Interactions and Their Applications, ed. L.G. Christophorou, Academic Press, New York, vol. 1 (1984).
[2] B. Boudaıffa *et al.*, Science **287** (2000) 1658.
[3] M. Kimura *et al.*, in Advances in Chemical Physics, I. Prigogine, S.A. Rice (Eds.),vol. LXXXIV, Wiley, (1993).
[4] M. Mucke *et al.*, Nature Phys. **6** (2010) 143.
[5] S. M. Pimblott and J.A. LaVerne, Radiat. Phys. Chem. **76** (2007) 1244.
[6] L. Sanche, Eur. Phys. J. D **35** (2005) 367.
[7] I. Baccarelli *et al.*, Phys. Rep. **508** (2011) 1.
[8] L. Sanche, Chem. Phys. Lett. **474** (2009) 1.
[9] J. Kopyra *et al.*, Phys. Chem. Chem. Phys. 16 (2014) 5342.
[10] J. Kopyra *et al.*, Phys. Chem. Chem. Phys. 16 (2014) 25054.

Dissociative ionization of Cyclopropylamine

M. Danko[1], P. Papp[1], Š. Matejčík[1]

[1]*Faculty of Mathematics, Physics and Inforamtics, Comenius University, Mlynská dolina F2,842 48 Bratislava,Slovakia*

Cyclopropylamine (CPA) is chemically most reactive cycloalkylamine. As such it is used in the manufacturing process of agrochemical active substances as an intermediate [1]. It has also its significant place in production of thin amine films by plasma deposition and polymerization techniques [2].

CPA was studied in a cross-beams experiment. Liquid sample was evaporated into a vacuum chamber through an effusive capillary, forming molecular beam. Electron beam of 200 meV FWHM energy distribution was formed in a trochoidal electron monochromator. Single collision conditions were met. Weak electric field was used for extraction of formed ions from the reaction region to the quadrupole mass spectrometer. The signal was detected by channeltron.

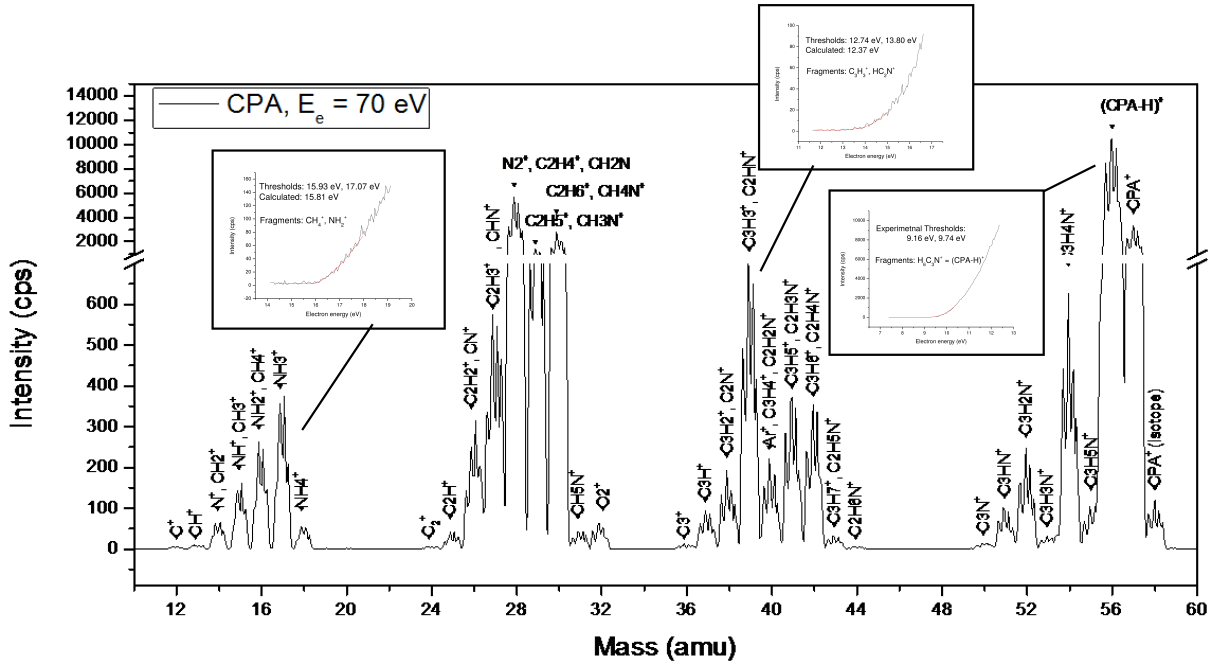

Figure 1: Mass spectrum of CPA

Mass spectrum of electron dissociative ionization products of CPA was measured at 70 eV of electron energy. The products were identified and cross section functions for all of them were measured. Threshold energies were estimated by fitting the measured functions using Wannier function. The experimentally estimated thresholds were compared to values calculated based on the enthalpy of creation of the dissociation products.

[1] Y. Shi *et al.*, J. Phys. Chem. A **118** (2014) 4484.
[2] A. Manakhov *et al.*, Plasma Processes and Polymers **11** (2014) 532.

Decomposition of nitroimidazoles by electron transfer

P. Limão-Vieira[1], M. Mendes[1,2], F. Ferreira da Silva[1], G. García[2]

[1]*Laboratório de Colisões Atómicas e Moleculares, CEFITEC, Departamento de Física, Universidade NOVA de Lisboa, 2829-516 Caparica, Portugal*

[2]*Instituto de Física Fundamental, Consejo Superior de Investigaciones Científicas (CSIC), Serrano 113-bis, 28006 Madrid, Spain*

Nitroimidazoles are a family of molecules that have been used in radiation therapy as radiosensitizers due to their ability to enhance the effect of ionising radiation in radioresistant hypoxic tumours [1,2], with particular relevance to nimorazole used in clinical trials in Danish hospital units for the treatment of head and neck cancers [2,3]. The underlying molecular mechanisms that lead to alteration of these species are triggered by electron interactions produced as secondary species along the ionization track of the primary radiation, so detailed knowledge on electron attachment and/or electron transfer processes are urgently needed. Dissociative electron attachment (DEA) processes on 4-nitroimidazole and methylated isomers [4,5] have reported that electrons with energies below 8 eV are capable of causing fragmentation [6,7]. The observation that high efficiency is achieved in neutral and radical anions formation even at ~ 0 eV, shows the relevance of exploring the mechanisms involved in these reactions, highlighting the implications to investigate new radiosensitizers compounds for tumour radiation therapy. However, Electron-transfer processes are predominant in several mechanisms and play relevant roles in a variety of environments within the biological environment [8]. Given this rationale, we have recently dedicated our research focus on electron transfer studies to nitroimidazoles.

In this presentation we show the most recent set of data on time-of-flight negative ion formation from collisions of potassium atoms with nitroimidazole targets and their methylated derivatives in a wide energy range. A part from the rich fragmentation pattern which seems to be relevant as to the role of reactions leading to the loss of NO, site- and bond-selective excision is demonstrated as a function of the collision energy [9].

MM and FFS acknowledge the Portuguese National Funding Agency FCT-MCTES through PD/BD/106038/2015 and researcher position IF-FCT IF/00380/2014, respectively, and together with PLV the research grant UID/FIS/00068/2013. This work was also supported by Radiation Biology and Biophysics Doctoral Training Programme (RaBBiT, PD/00193/2010); UID/Multi/ 04378/2013 (UCIBIO). GG acknowledges partial financial support from the Spanish Ministerio de Economia, Industria y Competitividad (Project No. FIS2016-80440).

[1] J. Overgaard and M. R. Horsman, Semin. Radiat. Oncol. **6** (1996) 10.
[2] J. Overgaard, Radiother. Oncol. **100** (2011) 22.
[3] M.A. Hassan Metwally *et al.*, Radiother. Oncol. **116** (2015) 15.
[4] L. Feketeová *et al.*, J. Phys. Chem. A **119** (2015) 9986.
[5] L. Feketeová *et al.*, Phys. Chem. Chem. Phys. **17** (2015) 12598.
[6] K. Tanzer *et al.*, J. Phys. Chem. A **119** (2015) 6668.
[7] K. Tanzer *et al.*, Angew. Chem. Int. Ed. Engl., **53** (2014) 12240.
[8] P. Limão-Vieira *et al.*, Electron Transfer-Induced Fragmentation in (Bio)Molecules by Atom-Molecule Collisions, Springer, 2012.
[9] M. Mendes *et al.*, in preparation.

Does Pinene stabilize water aerosols?

J. Kočišek[1], J. Poštulka[2], P. Slavíček[2], A. Domaracka[3], M. Fárník[1]

[1]*J. Heyrovský Institute of Physical Chemistry v.v.i., The Czech Academy of Sciences, Dolejškova 3, 18223 Prague 8, CZ*

[2]*Department of Physical Chemistry, University of Chemistry and Technology, Technická 5, Prague 6, CZ*

[3]*Centre de Recherche sur les Ions, les Matériaux et la Photonique CIMAP–CIRIL–GANIL, (CEA/CNRS/ENSICAEN/UCBN), Boulevard Henri Becquerel, BP 5133, F-14070 Caen, FR*

Terpenes are common precursors of secondary organic aerosols (SOA) [1]. These aerosols are important for temperature equilibrium of the Earth surface. Transformation of volatile terpenes to the aerosol nanoparticles is one of the open questions of the atmospheric chemistry. Theories explaining this process are based on the oxidation of terpenes on aerosol nanoparticles, photoionization or ionization by cosmic radiation [2].

In the present work we explore ionization of homogeneous α-pinene ($C_{10}H_{16}$) and mixed α-pinene-water clusters by electron impact. Studied neutral as well as ionic species can act as a model species for the atmospheric chemistry.

We observe signal enhancement at $n = 4$ in the mass spectra of the mixed cluster ions of the type $(C_{10}H_{16})_m(H_2O)_n^+$. Water tetramer cation is typical "magic" structure observed in the mass spectra of pure water clusters [3]. This indicates that the studied clusters have structure of the water cluster softly bound to pinene clusters. After ionization of pinene, the cluster is stabilized. Surprisingly, without dramatic chemical change of the constituents. On the other side, the ionization of water results in immediate α-pinene evaporation together with OH radical. Threshold electron ionization together with theory are combined to explore the observed behavior and identify its consequences for atmospheric chemistry.

Acknowledgement: This work was supported by the Czech Science Foundation grant no. 16-10995Y and MEYS Czech - French action Barrande 7AMB17FR047.

[1] M. Ehn *et al.*, Nature **506** (2014) 476.
[2] A.P. Praplan *et al.*, Atmos. Chem. Phys. **15** (2015) 4145;
F. Riccobono *et al.*, Science **344** (2014) 717.
[3] J. Kočišek *et al.*, J. Chem. Phys. **139** (2013) 214308.

Electron driven chemistry on comet 67P observed by Rosetta space craft and its implications

N. Mason[1]

[1]*School of Physical Sciences, The Open University, UK*

The European Space Agency Rosetta space craft orbited comet 67P between August 2014 and September 2016, exploring a regime not accessible before: the inner coma of a medium-activity comet at a large range of heliocentric distances. In contrast to expectations the observations from the Wide Angle Camera of the OSIRIS instrument revealed that emission observed in the OH, O I, CN, NH, and NH_2 filters is mostly produced by dissociative electron impact. This is the first time that an electron driven process is found to dominate the chemistry of a space borne object.

In this talk I will discuss these results and their implications for our knowledge of such processes in wider astrochemistry. I will discuss the current status of the data needed to analyse such data and how this may be expanded, both through experiment and theory, such that physical and chemical models of cometary systems may be developed. Finally I shall present the 'Grand challenges' facing both the cometary, astrochemistry and electron scattering communities that must be addressed through a collaborative research programme.

Abstracts of Posters

Low-energy resonant electron collisions with O_2

V. Alt[1], K. Houfek[1]

[1]*Insitute of Theoretical Physics, Faculty of Mathematics and Physics, Charles University, V Holešovičkách 2, 180 00, Praha 2*

Our interest lies in investigating nuclear dynamics of diatomic molecules in resonant collisions with electrons. This work specifically aims at calculating the cross sections for vibrational excitation of O_2 by an electron impact via the $^2\Pi_g$ resonance.

The process starts with obtaining the potential energy curves of O_2 and its negative ion. This was done by standard ab-initio quantum chemistry methods (CASSCF, MRCI – implemented in Molpro package [1]) under different conditions. Quality of the resulting curves was controlled by comparing calculated electron affinities with experimental values. The O_2 potential energy curve was additionally split due to the spin-orbital interaction which turned out to be essential for comparison with experiment. The resonant part of the O_2^- potential energy curve was calculated using the R-matrix method within the UKRmol suite of codes [2]. These calculations provide eigenphase sums and by fitting also the resonant energy and width.

Nuclear dynamics is then solved within the local complex potential approximation (LCP) [3] and compared with experimental data [4]. The LCP approximation however seems insufficient as it fails to reproduce the cross sections energy dependence properly. In future the nonlocal resonance model [5] will be used to treat the cross sections more thoroughly.

The study was supported by the Charles University, project GA UK No. 643216, and by the Grant Agency of Czech Republic under contract number GACR 16-17230S.

[1] H.J. Werner *et al.*, http://www.molpro.net.
[2] J.M. Carr *et al.*, Eur. Phys. J. D **66** (2012).
[3] L. Dubé and A. Herzenberg, Phys. Rev. A **20** (1979) 194.
[4] M. Allan, J. Phys. B **28** (1995) 5163.
[5] W. Domcke, Phys. Rep. **208** (1991) 97.

Absolute cross sections for photoionization of Ne^+ ions and Ne atoms in the vicinity of the K-shell ionization threshold

T. Buhr[1], D. Bernhardt[2], A. Borovik Jr.[1], J. Hellhund[2], K. Holste[1], A. L. D. Kilcoyne[3], S. Klumpp[4,5], M. Martins[4], S. Ricz[6], J. Seltmann[7], J. Viefhaus[7], S. Schippers[1], A. Müller[2]

[1]*I. Physikalisches Institut, Justus-Liebig-Universität Gießen, 35392 Gießen, Germany*

[2]*Institut für Atom- und Molekülphysik, Justus-Liebig-Universität Gießen, 35392 Gießen, Germany*

[3]*Advanced Light Source, Lawrence Berkeley National Laboratory, CA 94720 Berkeley, USA*

[4]*Institut für Experimentalphysik, Universität Hamburg, 22761 Hamburg, Germany*

[5]*DESY Photon Science, FS-FLASH-D, 22607 Hamburg, Germany*

[6]*Institute for Nuclear Research, Hungarian Academy of Sciences, 4001 Debrecen, Hungary*

[7]*DESY Photon Science, FS-PE, 22607 Hamburg, Germany*

Absolute cross sections for photoionization of Ne^+ ions and neutral Ne atoms have been experimentally determined in the photon energy range of 840 eV to 930 eV covering the lowest-energy resonances containing K-shell excitations as well as double excitations involving K- and L-shell electrons [1].

The measurements were carried out at the PIPE setup [2] at the beam line P04 on the synchrotron light source PETRA III (Hamburg, Germany) employing the photon-ion merged-beams technique. The PIPE setup (Photon-Ion Spectrometer at PETRA III) [2] is an experimental facility for investigating photon-charged particle interactions. The photon energy bandwidths were chosen between 32 meV and 500 meV enabling the determination of the natural line widths of several prominent lines associated with K-vacancy levels in neutral Ne atoms and Ne^+ ions. The uncertainty of the energy scale is approximately 0.2 eV.

In case of Ne^+ ions, single, double and triple photoionization by a single photon have been studied. Transition probabilities and branching ratios could be determined for the decay of K-vacancy levels. From the analysis the fluorescence yield of Ne K_α radiation has been determined and the presence of complex many-electron Auger-decay mechanisms has been revealed. For comparison with theoretical models, photoabsorption cross sections were inferred by summing the measured partial ionization channels.

For neutral Ne atoms, electron production associated with single-photon absorption has been investigated. By normalizing the electron-emission spectra, absolute cross sections for photoelectron production and for photoabsorption were derived.

Funding by the Bundesministerium für Bildung und Forschung (BMBF, Grant numbers: 05K10RG1, 05K10GUB, 05K16RG1, 05K16GUC and 05K16SJA) is gratefully acknowledged. SK acknowledges support from the European Cluster of Advanced Laser Light Sources (EUCALL) project which has received funding from the European Union's Horizon 2020 research and innovation program (Grant No.: 654220). We would like to thank the staff of the beam line P04 for their valued support.

[1] A. Müller *et al.*, Astrophysical Journal **836** (2017) 166.
[2] S. Schippers *et al.*, J. Phys. B **47** (2014) 115602.

Isotope effect in water formation by associative detachment

M. Čížek[1], K. Houfek[1], J. Táborský[1]

[1]*Institute of Theoretical Physics, Faculty of Mathematics and Physics, Charles University, V Holešovičkách 2, Prague*

Water is one of the most abundant and most important molecules in nature. Despite of this, many elementary processes including this molecule are not well understood. This includes creation of water molecule by associative detachment process

$$H_2 + O^- \rightarrow H_2O + e \tag{1}$$

Recent experiments [1] with oxygen anion in the 22-pole trap measured reaction rates for both associative detachment reaction (1) and hydrogen transfer reaction

$$H_2 + O^- \rightarrow OH^- + H \tag{2}$$

for temperatures $10 - 300$ K. The associative detachment reaction was found to be very efficient exceeding Langevin rate by several percent. This is in contrast with higher temperatures measured previously, were the rate was one third of the Langevin value. The hydrogen transfer rate was more than one order of magnitude smaller.

In order to explain these measurements we constructed full 3D potential energy surface for lowest three water anion states in all regions relevant to reactions (1) and (2) at low temperatures. The potential energy surface was interpolated from more than 50000 points calculated with MRCI method using aug-cc-pVTZ basis. Davidson correction was also included. We also determined the electron auto-detachment region by calculation the potential for the neutral water molecule.

Using the lowest of the anion potentials we calculated the reaction rates employing the classical-trajectory Monte Carlo method. The results agree qualitatively well with the experimental data [1]. In this work we extend the calculation also for collisions of O^- anion with D_2 and HD molecules. It turns out that the associative detachment reaction is rather insensitive to the isotope substitution. The hydrogen (deuterium) transfer reaction is much more sensitive. The reaction rate for the deuterated analog of the reaction (2) is five times smaller than the hydrogen case. Surprising result is found for the case of HD molecule. The reaction rate for OH^-+D channel is three times larger than OH^-+H reaction rate and OD^-+H rate is slightly smaller than OD^-+D reaction rate. These results may have important consequences for isotopic composition of the interstellar molecular clouds.

The calculated water anion potential energy surface is also relevant for the description of the electron-water-molecule collisions. As a step in this direction we have calculated [2] low-energy fixed nuclei electron scattering eigenphases using the London R-matrix suite of codes.

Preliminary results demonstrating chaos emerging in the classical-trajectory simulation of the O^-+H_2 collisions are also shown in this contribution.

[1] Jusko *et al.*, J. Chem. Phys. **142** (2015) 014304.
[2] Houfek and Čížek, Eur. Phys. J. D **70** (2016) 107.

Elastic electron scattering by the CF_3 radical and by the CF_3Cl, CF_4 molecules in the IAM approach

S. Demes[1], V. Kelemen[2], E. Remeta[2]

[1]*Institute for Nuclear Research, Hungarian Academy of Sciences (ATOMKI), Bem square 18/c, 4026 Debrecen, Hungary*

[2]*Institute of Electron Physics NASU, Universitetska St. 21, 88017 Uzhhorod, Ukraine*

The behaviour of differential (DCSs) and integral (ICSs) cross sections of elastic electron scattering by the CF_3 radical and by the CF_3Cl, CF_3H and CF_4 molecules were studied at 10, 20, 30, 50 and 100 eV energies in the framework of independent atom model (IAM). Two approximations are used: the Additive Rule (AR, which corresponds to the optical theorem) and the IAM (see [1]). In order to calculate the atomic scattering amplitudes we use the real or the complex optical potential (OP) methods. The real parts of the OP for the C, F and Cl atoms are parameter-free and consist of the following potentials: scalar-relativistic and spin-orbit coupling, static, local exchange and polarization (RSEP-approximation) [1]. The Hartree-Fock electron densities are used for the C, F and Cl atoms [2]. The inelastic effects of electron-atom scattering (RSEPA-approximation) are taken into consideration by the Staszewska-type absorption potential. The equilibrium interatomic distances are calculated by geometry optimization with the GAUSSIAN software package at the CCSD(T) level of theory.

The calculated DCSs are compared with different experimental data for $e + CF_3$ [3] (•••), $e + CF_4$ [4] (○○○), $e + CF_3H$ [5] (×××) and $e + CF_3Cl$ [6] (□□□) scattering (see Fig.1). Fig.1. shows the essential influence of the chlorine atom for the DCSs of the CF_3Cl molecule as compared with the CF_3 radical and with the CF_4 molecule.

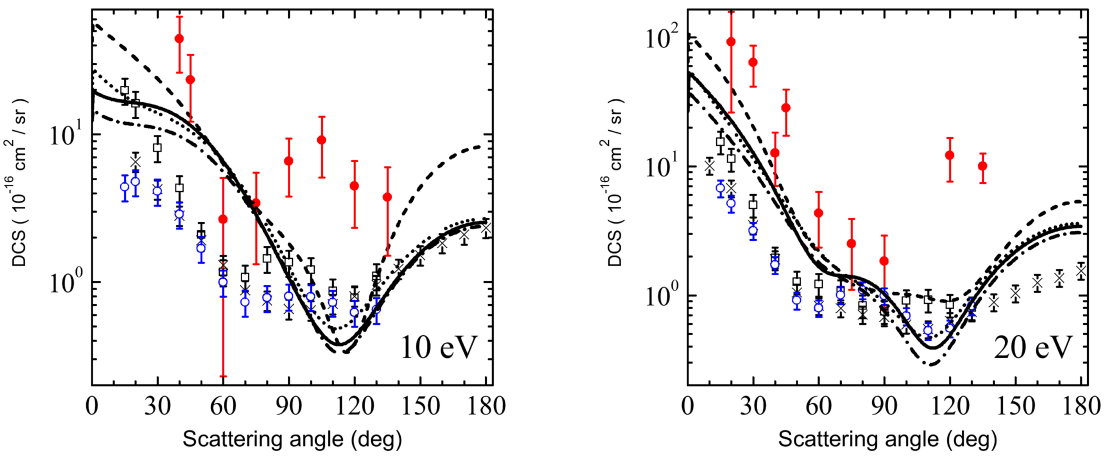

Figure 1: DCSs for $e + CF_3$ (−·−·−), CF_3Cl (− − −), CF_3H (···) and CF_4 (—) scattering at 10 and 20 eV.

[1] Sh. Demesh *et al.*, J. Phys. B **50** (2017) 135201.
[2] T.G. Strand and R.A. Bonham, J. Chem. Phys. **40** (1964) 1686.
[3] J.R. Brunton *et al.*, J. Phys. B **46** (2013) 245203.
[4] J.-S. Yoon *et al.*, Phys. Chem. Ref. Data. **39** (2010) 033106.
[5] H. Cho *et al.*, J. Phys. B **43** (2010) 135205.
[6] K. Sunohara *et al.*, J. Phys. B **36** (2003) 1843.

IAM approach study of elastic electron scattering by the CF_2, CF_2Cl and CF_3 molecular systems

S. Demes[1], V. Kelemen[2], E. Remeta[2]

[1]*Institute for Nuclear Research, Hungarian Academy of Sciences (ATOMKI), Bem square 18/c, 4026 Debrecen, Hungary*

[2]*Institute of Electron Physics NASU, Universitetska St. 21, 88017 Uzhhorod, Ukraine*

The behaviour of differential (DCSs) and integral (ICSs) cross sections of elastic electron scattering by the CF_2, CF_2Cl and CF_3 radicals were studied at 10, 15, 20, 25, 30, 35, 40, 50 and 100 eV energies in the framework of independent atom model (IAM). Two approximations are used: the Additive Rule (AR, which corresponds to the optical theorem) and the IAM (see [1]). In order to calculate the atomic scattering amplitudes we use the real or the complex optical potential (OP) methods. The real parts of the OP for the C, F and Cl atoms are parameter-free and consist of the following potentials: scalar-relativistic and spin-orbit coupling, static, local exchange and polarization (RSEP-approximation) [1]. These components are determined by the total electron densities of the atomic components of the molecule. The Hartree-Fock electron densities are used for the C, F and Cl atoms [2]. The inelastic effects of electron-atom scattering (RSEPA-approximation) are taken into consideration by a non-empirical absorption potential [3]. The equilibrium interatomic distances for all molecules are calculated by geometry optimization with the GAUSSIAN software package at the CCSD(T) level of theory. The calculated DCSs are compared with experimental data for $e + CF_3$ [4] (• • •) and $e + CF_2$ [5] (○ ○ ○) scattering (see Fig.1). Fig.1. shows the influence of the chlorine atom for the DCSs of the CF_2Cl molecule as compared with the CF_2 and CF_3 radicals.

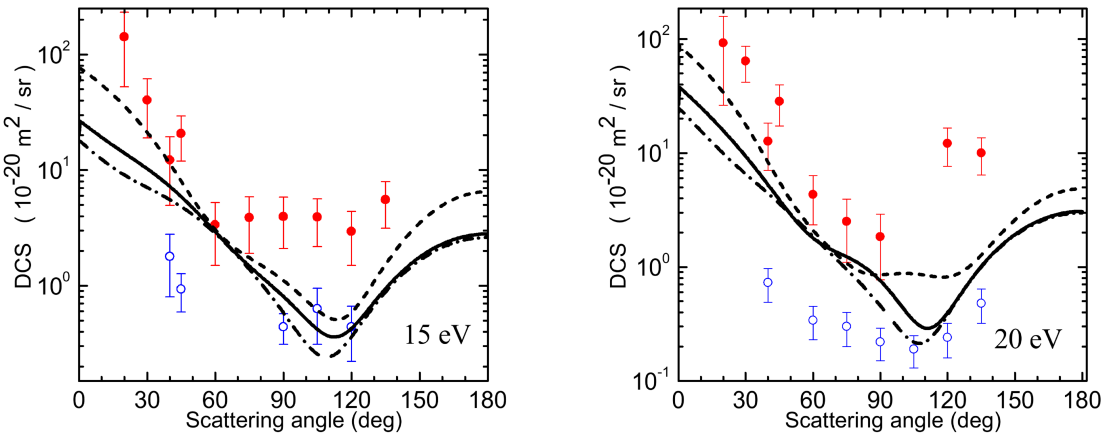

Figure 1: DCSs for $e + CF_2$ ($- \cdot - \cdot -$), CF_2Cl ($- - -$), CF_3 (—) scattering at 15, 20 eV (RSEPA theory).

[1] Sh. Demesh *et al.*, J. Phys. B **50** (2017) 135201.
[2] T.G. Strand and R.A. Bonham, J. Chem. Phys. **40** (1964) 1686.
[3] G. Staszewska *et al.*, Phys. Rev. A **29** (1984) 3078.
[4] J.R. Brunton *et al.*, J. Phys. B **46** (2013) 245203.
[5] J.-S. Yoon *et al.*, Phys. Chem. Ref. Data. **39** (2010) 033106.

Double electron capture by the O^{2+} projectile in collisions with the H_2 molecule

S. Demes[1], S.T.S. Kovács[1], P. Herczku[1], Z. Juhász[1], E. Bene[1], J.-Y. Chesnel[2], A. Méry[2], J. Rangama[2], V. Vizcaino[2], B. Sulik[1]

[1]*Institute for Nuclear Research, Hungarian Academy of Sciences (ATOMKI), Bem square 18/c, 4026 Debrecen, Hungary*

[2]*Centre de Recherche sur les Ions, les Matériaux et la Photonique (CIMAP), Unité mixte CEA-CNRS-Ensicaen-Université de Caen Basse-Normandie, UMR 6252, 6 Boulevard Maréchal Juin, F-14050 Caen cedex 04, France*

Energy and angular distribution of H^+ fragments and ejected electrons were measured by 10 and 30 keV O^{2+} impact on H_2 target in a conventional crossed-beam arrangement. Special attention was devoted to the angular distribution of the fragments. The measured angular anisotropy in the fragment energy spectra is to be compared with the results of coupled-channel calculations. Electrons from the double electron capture into excited states of the projectiles followed by autoionization also contributed to the electron emission spectra. The appearing autoionization peaks carry detailed information about the precursor excited states as well as the electronic rearrangements of the excited projectile.

Theoretical calculations were performed in order to describe the angular anisotropy observed in the measured cross sections of double electron capture by the O^{2+} projectile at different collision energies. The lowest $^3\Pi$ and $^3\Sigma^-$ states of the $O^{2+} + H_2$ system were calculated by the MOLPRO program package [1] at the CASSCF+MRCI level of theory in order to obtain the potential energy curves and the radial coupling matrix elements between all pair of states. The collision dynamics was modelled by a semiclassical approach using the EIKONXS code [2]. The calculated cross sections of the double electron capture for different orientations of the H_2 molecular target are shown in Fig. 1.

Supported by the Hungarian-French S&T collaboration (TÉT_16-1-2016-0126), the Hungarian NKFIH-OTKA project (Gr. No. K109440) and the IVF EaP (Gr. No. 51600934).

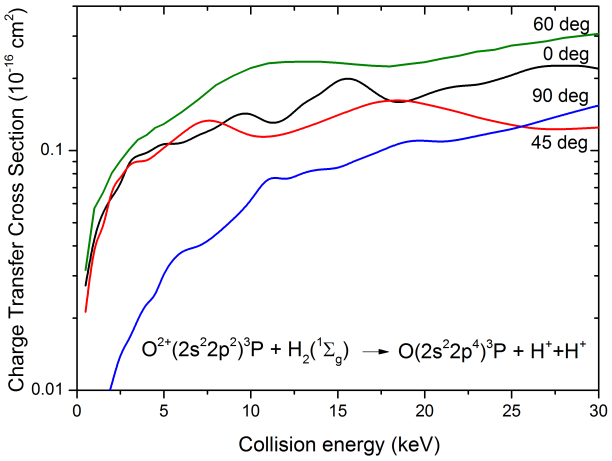

Figure 1: Charge transfer cross sections for different orientations of the H_2 molecule with respect to the O^{2+} projectile's velocity.

[1] H.J. Werner and P. Knowles, MOLPRO package of *ab initio* programs (2010).
[2] R.J. Allan *et al.*, J. Phys B **23** (1990) L461.

Dissociative electron attachment (0-9 eV) to D-ribose molecule

I.V. Chernysova[1], J.E. Kontrosh[1], O.B. Shpenik[1], P.P. Markush[1], S. Demes[2]

[1]*Institute of Electron Physics NASU, 21 Universitetska St., 88017, Uzhhorod, Ukraine*

[2]*Institute for Nuclear Research, Hungarian AS, Bem square 18/c, 4026 Debrecen, Hungary*

In this work the total cross-section of dissociative electron attachment to D-ribose molecule in the gas phase in the energy region 0-9 eV has been studied using hypocycloidal electron spectrometer [1]. It is important to note that until now the dissociative electron attachment to D-ribose molecule has been investigated exclusively by massspectroscopy method [2].

D-ribose ($C_5H_{10}O_4$)-pentose monosaccharide with 5C atoms. This molecule is part of the building blocks that form DNA and RNA molecules. Studies of the last decade have shown that during interaction of high-energy radiation with living matter slow electrons are produced which can cause damages to it. Therefore the study of interaction of slow electrons with D-ribose is relevant. In the figure 1 the total

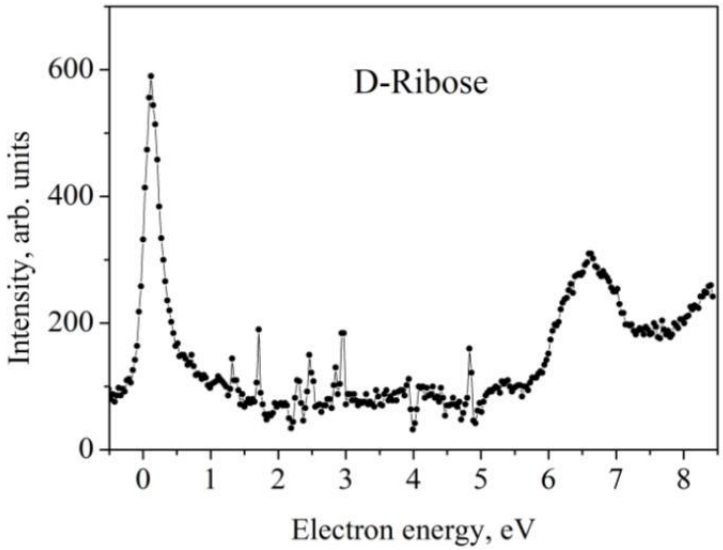

Figure 1: Total cross-section of dissociative electron attachment to D-ribose molecule.

cross-section of dissociative electron attachment to D-ribose molecule measured in the electron energy region of 0-9 eV and at temperature of 80°C is shown. In the curve an intense peak at near zero energy and a low intense maximum in the energy region 0f 6-8 eV can be observed. Based on the results of work [2] we assume that the observed features appear due the formation of $C_5H_8O_4^-$, $C_5H_6O_3^-$, $C_4H_5O_3^-$, $C_3H_4O_2^-$, $C_3H_3O_2^-$, $C_2H_3O_2^-$ and OH^- fragment ions by dissociative electron attachment to D-ribose molecule.

[1] J.E. Kontros *et al.*, J. Phys. B: At. Mol. Opt. Phys. **35** (2002) 2195.
[2] I. Baccarelli *et al.*, J. Am. Chem. Soc. **129** (2007) 6269.

Electron impact excitation of the gas-phase ribose molecule

M.M. Erdevdy[1], O.B. Shpenik[1], P.P. Markush[1], S. Demes[2]

[1]*Institute of Electron Physics NASU, 21 Universitetska St., 88017, Uzhhorod, Ukraine*

[2]*Institute for Nuclear Research, Hungarian AS, Bem square 18/c, 4026 Debrecen, Hungary*

Ribose is a sugar alcohol, which can be obtained by glucose reduction, changing the aldehyde group to a hydroxyl group. Sugars and sugar alcohols being considered as biobased feedstocks to produce many of the chemicals in common use, which are derived from petroleum feedstocks [1]. Utilization of biobased materials will help to overcome energy shortage and prevent serious environmental pollution. This work has been devoted to the investigation of electron impact excitation of ribose in the gas phase.

This study was carried out by using a gas-filled cell at incident electron current of 30 μA provided by a four-electrode gun with an oxide coated cathode [2]. Radiation selected by a diffraction monochromator MDR-2 was detected by a FEU-106 photomultiplier. Fig. 1 shows the emission spectra of the ribose

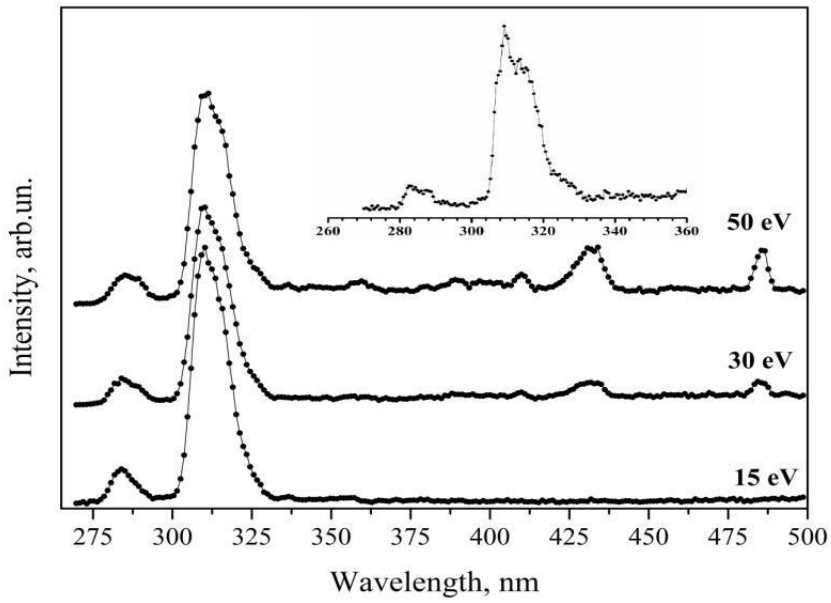

Figure 1: Ribose emission spectra, the inset shows the region 260-360 nm measured with smaller step and longer exposition time.

molecule measured in the wavelength range between 270-500 nm at the incident electron energies of 15, 30 and 50 eV. As seen, the spectra are relatively poor, only several bands and one line can be observed. We assume that the bands with the maxima between 280-290 nm and 308-324 nm are resulted from the excited OH radical (transition: $X^2\Pi - A^2\Sigma^+$) [3]. As for the band with maximum between 425-440 nm it most probably forms due to the CH group emission (transition: $A^2\Delta - X^2\Pi$). In our opinion the spectral line at 486 nm is related to the excitation of the H atom.

We also measured the optical excitation function for the bands as well the line and determined their threshold energies.

[1] Y. Wand and J. Suppes, J. Chem. Eng. Data. **53** (2008) 2033.
[2] O.B. Shpenic *et al.*, J. Appl. Spect. **80** (2013) 46.
[3] M.T.I. Soskyda, Uzhgorod University Scientific Herald Series Physics **30** (2004) 54.

Ion guiding through a macroscopic capillary: A quantitative study

R.D. DuBois[1], E. Giglio[2], K. Tökési[3,4]

[1]*Missouri University of Science and Technology, Rolla MO 65409 USA*

[2]*Centre de Recherche sur les Ions, les Matériaux et la Photonique (CIMAP), F-14000, Caen, France, EU*

[3]*Institute for Nuclear Research, Hungarian Academy of Sciences (ATOMKI), Hungary, EU*

[4]*ELI-ALPS, ELI-HU Non-profit Kft., Dugonics tér 13, H-6720 Szeged, Hungary, EU*

Charged particle guiding has been of interest for a long time, however little or no information about the actual capillary charge is available. The present study helps to fill this void by studying the transmission of single charged 1 keV Ar ions through a macroscopic cylindrical glass capillary. In this work, quantitative measurements of the incoming and transmitted beams include scanning the beam across the entrance of the capillary and measuring the time evolution of the guided beam following various times during which the capillary was allowed to discharge. The scanning measurements provided information about the current entering the capillary while the temporal studies provided information about the charging and discharging rates plus the amount of current deposited as a function of time. These were used to model the residual capillary charge as a function of time for fully, and partially, discharged conditions (see Fig. 1). Doing so enabled us to compress the transmission curves measured for a wide range of discharge times to a single curve for the guiding probability as a function of capillary charge. Findings from this study imply that during beam injection only a portion of the deposited charge contributes to the guiding phenomenon and that for measurements involving a partially discharged capillary the initial charge is determined from the slow decay of much, but not all, of the charge deposited in a previous run.

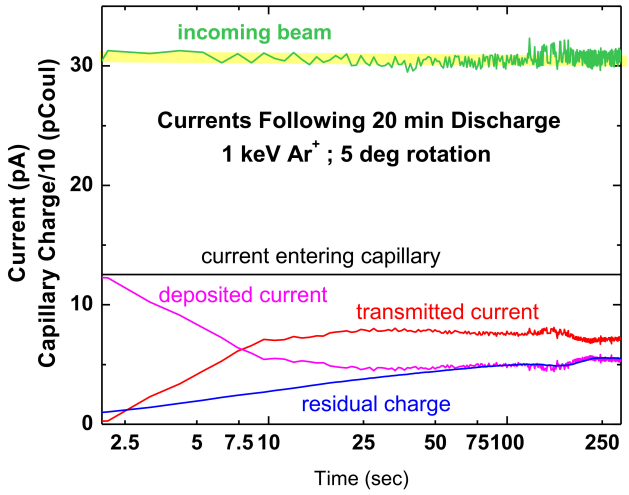

Figure 1: Time dependences for the incoming, transmitted, and deposited currents and for the residual charge when 1 keV Ar^+ ions passing through a cylindrical glass capillary at 5° tilt angle.

This work was funded by the French National Research Agency (ANR) in the P2N 2012 program (ANR-12-NANO-008) for the PELIICAEN project, and by the European Cost Actions CM1405 (MOLIM) and MP1306 (MPNS).

Electron scattering cross section data for tungsten and beryllium atoms from 0.1 to 5000 eV

F. Blanco[1], F. Ferreira da Silva[2], P. Limão-Vieira[2], G. García[3]

[1]*Departamento de Física Atómica, Molecular y Nuclear, Universidad Complutense de Madrid, Avenida Complutense, 28040 Madrid, Spain*

[2]*Laboratório de Colisões Atómicas e Moleculares, CEFITEC, Departamento de Física, Universidade NOVA de Lisboa, 2829-516 Caparica, Portugal*

[3]*Instituto de Física Fundamental, Consejo Superior de Investigaciones Científicas (CSIC), Serrano 113-bis, 28006 Madrid, Spain*

Tungsten (W) and tungsten-based materials have been widely recognized for their distinctive and suitable thermophysical properties well attuned to fusion applications [1, 2]. However, electron scattering data for these materials are scarce.

In this study, we report integral cross sections (ICS) for electron interactions with tungsten and beryllium atoms in the incident electron energy range from 0.1 up to 5000 eV. The calculated cross sections are obtained for electron–atom scattering processes represented by a complex potential. For tungsten, ionization cross sections are discussed in the electron energy region from threshold up to 5000 eV against the available data from the Deutsch–Märk (DM) formalism [3] and a semi-empirical complex scattering potential [4]. Although a reasonable agreement for the ionization cross sections has been found in the overlapping energy region, inconsistencies on the integral inelastic cross sections from the previous semi-empirical approach based on a complex scattering potential ionization contribution [4], are now amended and comprehensively explained. For beryllium atoms an excellent agreement with previous "state-of-the-art" scattering theory calculations [5] has been found for the integral elastic cross sections. However, the partial contribution of the excitation and ionization channels to the inelastic part shows serious discrepancies which deserve further investigations. Calculated elastic differential cross sections (DCSs) for tungsten are also reported from 0.1 to 5000 eV for scattering angles from 0° to 180°. The present set of cross sectional data may be of relevance for the plasma fusion community.

MM and FFS acknowledge the Portuguese National Funding Agency FCT-MCTES through PD/BD/106038/2015 and researcher position IF-FCT IF/00380/2014, respectively, and together with PLV the research grant UID/FIS/00068/2013. This work was also supported by Radiation Biology and Biophysics Doctoral Training Programme (RaBBiT, PD/00193/2010); UID/Multi/ 04378/2013 (UCIBIO). GG acknowledges partial financial support from the Spanish Ministerio de Economia, Industria y Competitividad (Project No. FIS2016-80440).

[1] S. Wurster *et al.*, J. Nucl. Mater. **442** (1913) S181.
[2] J. Riesch *et al.*, Nucl. Mater. Energy **9** (2016) 75; M.A. Hassan Metwally *et al.*, Radiother. Oncol., **116** (2015) 15.
[3] H. Deutsch *et al.*, J. Appl. Phys. **89** (2001) 1915.
[4] B. Goswami *et al.*, Int. J. Mass Spectrom. **372** (2014) 8.
[5] O. Zatsarinny *et al.*, J. Phys. B: At. Mol. Opt. Phys. 49 (2016) 235701.

Analysis of two theoretical methods for dissociative recombination of small cations

D. Hvizdoš[1,2], R. Čurík[1], M. Váňa[2], K. Houfek[2], C.H. Greene[3], T.N. Rescigno[4], C.W. McCurdy[4,5]

[1]*J. Heyrovský Institute of Physical Chemistry, ASCR, Dolejškova 3, 18223 Prague, Czech Republic*

[2]*Institute of Theoretical Physics, Faculty of Mathematics and Physics, Charles University in Prague, V Holešvičkách 2, 180 00 Prague, Czech Republic*

[3]*Department of Physics and Astronomy, Purdue University, West Lafayette, Indiana 47907, USA*

[4]*Chemical Sciences Division, Lawrence Berkeley National Laboratory, Berkeley, California 94720, USA*

[5]*Department of Chemistry, University of California, Davis, California 95616, USA*

Dissociative recombination (DR) is a highly important but complicated process of molecular plasma dynamics. Unfortunately, exact models of this phenomenon are quite hard to work with, so when calculating DR cross sections, approximative methods are used instead and exact results exist for only the simplest cases.

A common approximative approach is to take the well-established frame transformation method [1] typically used to model rovibrationally inelastic collisions of electrons with neutral molecules and adapt it to the case of DR. This has been done for the case of H_2^+, H_3^+, LiH^+, HeH^+, NO_2^+ and $LiHe^+$, using Siegert states for the nuclear vibrational basis. All the previous studies that use this method contain several non-trivial intuitive or ad-hoc assumptions to obtain the DR cross sections and so the validity of their use could be called into question. The goal of our current project is to provide theoretical and numerical evidence to confirm or disprove these assumptions for the simple case of H_2^+ DR. Our poster will present how the results of the aforementioned approximative method hold up when compared with the results from an alternative method which solves the model two-dimensional Hamiltonian in a numerically exact manner [2].

[1] E.S. Chang and U. Fano., Phys. Rev. A **6** (1972) 173.
[2] K. Houfek *et al.*, Phys. Rev. A **73** (2006).

Thermodynamic model of molecular collisions

Z. Juhász[1]

[1]*Institute for Nuclear Research, Hungarian Academy of Sciences (MTA Atomki), P.O. Box 51, H-4001 Debrecen, Hungary*

A statistical-type model is developed to describe the ion production and electron emission in collisions of (molecular) ions with atoms or molecules [1]. The model is based on the Boltzmann population of the bound electronic energy levels of the quasi molecule formed in the collision and the discretized continuum. The discretization of the continuum is implemented by a free electron gas in a box model assuming an effective square potential of the quasi molecule. The temperature of the electron gas is calculated by taking into account a thermodynamically adiabatic process due to the change of the effective volume of the quasi molecule as the system evolves. The system may undergo a transition with a small probability from the discretized continuum to the states of the complementary continuum, that is an electron is ejected from the system. It is assumed that state of the residual quasi molecule is decoupled from the thermodynamic time development. The dissociation limit of this state determines the asymptotically observed fragment ions emitted from the collision. The first motivation of this work was to describe the recently observed H^- ion production in OH^++Ar collisions [2,3]. The obtained differential cross sections for H^- formation, cation production and electron emission are close to the experimental ones. Calculations for the atomic systems O^++Ar and H^++Ar are also in reasonable agreement with the experiments (see Fig. 1) indicating that the model can be applied to a wide class of collisions.

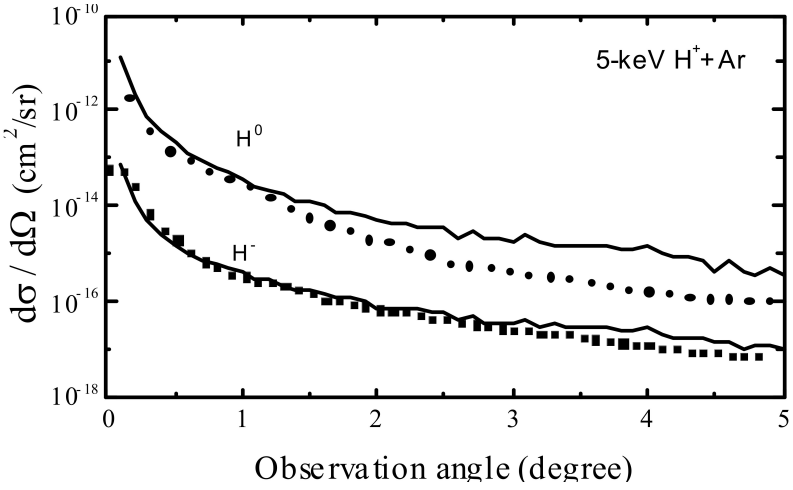

Figure 1: Single differential cross sections according to observation angle for H^- (quares) and H^0 (circles) production for 5-keV H^++Ar collisions [4,5]. Lines belong to the theory.

National Information Infrastructure Development Institute (NIIF) is acknowledged for awarding access to resource based in Hungary at Szeged. This work was supported by the Hungarian National Science Foundation OTKA (Grant No. K109440).

[1] Z. Juhász, Phys. Rev. A **94** (2016) 022707.
[2] Z. Juhász *et al.*, Phys. Rev. A **87** (2013) 032718.
[3] E. Lattouf *et al.*, Phys. Rev. A **89** (2014) 062721.
[4] F.B. Alarcon *et al.*, AIP Conf. Proc. **1099** (2009) 184.
[5] H. Martinez *et al.*, Phys. Rev. A **78** (2008) 062715.

DNA binding radiosensitizers and low energy electrons

J. Kočišek[1], D. Reimitz[1,2], J. Fedor[1], M. Fárník[1], J. Pinkas[1], M. Davídková[3]

[1]*J. Heyrovský Institute of Physical Chemistry v.v.i., The Czech Academy of Sciences, Dolejškova 3, 18223 Prague 8, CZ*

[2]*Faculty of Nuclear Sciences and Physical Engineering, Czech Technical University in Prague, Břehová 7,115 19 Prague, CZ*

[3]*Nuclear Physics Institute of the CAS, Na Truhlářce 39/64, 180 00 Prague, CZ*

During the interaction of ionizing radiation with living matter, a number of secondary species is formed. One of such species are low energy (0 eV - 10 eV) electrons. These electrons are formed in a large amount and exhibit energy dependent, resonant, breakage of DNA [1]. The resonant process that leads to the bond breaking at these low electron energies is called dissociative electron attachment (DEA). Several radiosensitizers exhibit large cross sections for the DEA, what was used as a base for the description of a synergistic effect of the combined chemo – radiation therapy. That is the higher combined effect of radiation and chemotherapy in comparison to the additive effect of individual treatments. The effect was studied for DNA binding chemotherapeutics such as cisplatin [2] or halo-uracils [3].

In this contribution, we present our experimental studies of cisplatin and halouracils in the effort to explain fundamentals of the synergistic effect. First, we are studying the DEA in clusters that mimic effects of an environment on such interaction (e.g. [4]). Second, we are studying the damage caused to DNA by high energy ionizing radiation (e.g. [5]), which can identify a relative importance of the low energy electrons. Our studies show that direct effects of low energy electrons are low and more complex chemical and bio-chemical models need to be developed to explain the chemo – radiation synergy observed in vivo.

Acknowledgment: This work was supported by the Czech Science Foundation (grant No.16-10995Y).

[1] B. Boudaiffa *et al.*, Science **287** (2000) 1658.
[2] M. Rezaee *et al.*, Int. J. Radiat. Oncol. Biol. Phys. **87** (2013) 847.
[3] L. Chomicz*et al.*, J. Phys. Chem. Lett. **4** (2013) 2853.
[4] J. Kočišek *et al.*, J. Phys. Chem. Lett. **7** (2016) 3401.
[5] D. Reimitz *et al.*, Radiation Physics and Chemistry **141** (2017) 229.

Electron emission mechanisms in ion-induced ionization of small molecules

S.T.S. Kovács[1], P. Herczku[1], L. Sarkadi[1], L. Gulyás[1], Z. Juhász[1], B. Sulik[1]

[1]*Institute for Nuclear Research, Hungarian Academy of Sciences (MTA Atomki), Bem tér 18/c, 4026 Debrecen, Hungary*

Ionization of atoms and molecules is of fundamental interest in atomic and molecular physics [1] as well as in applied fields for instance plasma physics, industrial irradiations and radiotherapy. In this work ion-impact induced ionization of small molecules is investigated both experimentally and theoretically.

In the experiments gas phase CH_4, H_2O and N_2 molecules were bombarded by 46-1000 keV/u H^+, He^+, C^+ and N^+ ions. Electron energy spectra were taken by an energy-dispersive electrostatic spectrometer in the 20°-160° observation angle range. Absolute double-differential electron-emission cross sections (DDCS) have been determined.

The experimental results were compared with the predictions of the extended CDW-EIS and CTMC models [2]. The perturbative quantum mechanical CDW-EIS method was extended for dressed projectiles and molecular targets. In our classical CTMC calculations we used a multi-center approach with a full three-body dynamics. This model is very similar to that of Illescas *et al.* [3]. In Figure 1 we compare the

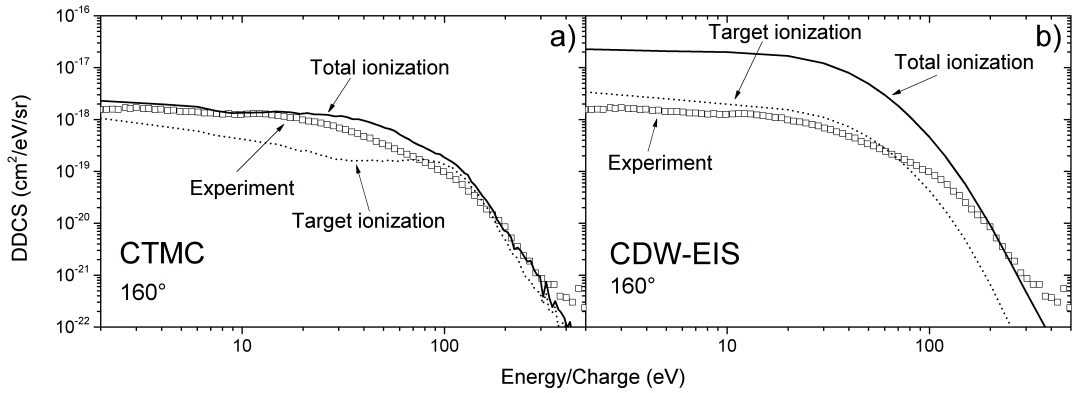

Figure 1: Comparison of the experimental electron spectrum with the results of CTMC (a) and CDW-EIS (b) calculations at 160° observation angle for 650 keV N^++H_2O collisions.

energy spectrum of the electrons ejected in 46 keV/u N^++H_2O collisions at 160° observation angle with CTMC (figure 1a) and CDW-EIS [4] (figure 1b) calculations. A good overall agreement was found between the experimental DDCS and the total ionization curve (comparable with the experiments) obtained by the non-perturbative CTMC calculations. The CDW-EIS overestimates both the projectile and target contributions below c.a. 80 eV. Above this electron energy the CDW-EIS results fall off significantly faster then the experimental data. The calculated target ionization fraction is also shown in the figure.

By comparing the results of the non-perturbative CTMC model with 1st order Born reference calculations we interpreted the major electron emission mechanism in the measured spectra, including some higher order processes. Accordingly, the peak-like structure above c.a. 100 eV is due to multiple electron scattering i.e., the Fermi-shuttle mechanism [4].

This work was supported by the Hungarian National Science Foundation OTKA (Grant No. K109440).

[1] A.N. Agnihotri *et al.*, Phys. Rev. A **87**, 032716 (2013).
[2] S.T.S. Kovács *et al.*, Phys. Rev. A **94**, 012704 (2016).
[3] C. Illescas *et al.*, Phys. Rev. A **83**, 052704 (2011).
[4] B. Sulik *et al.*, Phys. Rev. Lett. **88**, 073201 (2002).

Nd:YAG laser ablation of materials of biological interest

M.S. Rabasović[1], D. Sevic[1], B.P. Marinković[1]

[1]*Institute of Physics Belgrade, University of Belgrade, Serbia*

The aim of this study is to analyze the possibilities of using of the Laser Induced Breakdown Spectroscopy (LIBS) for discerning the materials ablated by laser. Lasers are widely used for ablation of biological materials. For practical considerations in biomedical applications, it is necessary to have a real-time feedback control system, so that discriminating between the ablated layers is possible. As excitation laser we use Nd:YAG (1064 nm, pulse width 5 ns, energy up to 300 mJ). We used dry pork bone as an experimental sample. The diagnostic part of our experiment is based on streak camera, so we can perform the time resolved analysis of spectral data. Reasoning of our LIBS analysis follows the concept presented in [1], where femtosecond laser was used for tissue ablation. Sodium (Na) line at 589 nm and Calcium (Ca) line at 612 nm could be used for discrimination between the soft tissue and the bone. Nanosecond Nd:Yag lasers are also widely used for biomedical applications [2,3] Our method of time resolved LIBS is presented in [4]. This study was inspired by a similar analysis (not for biological

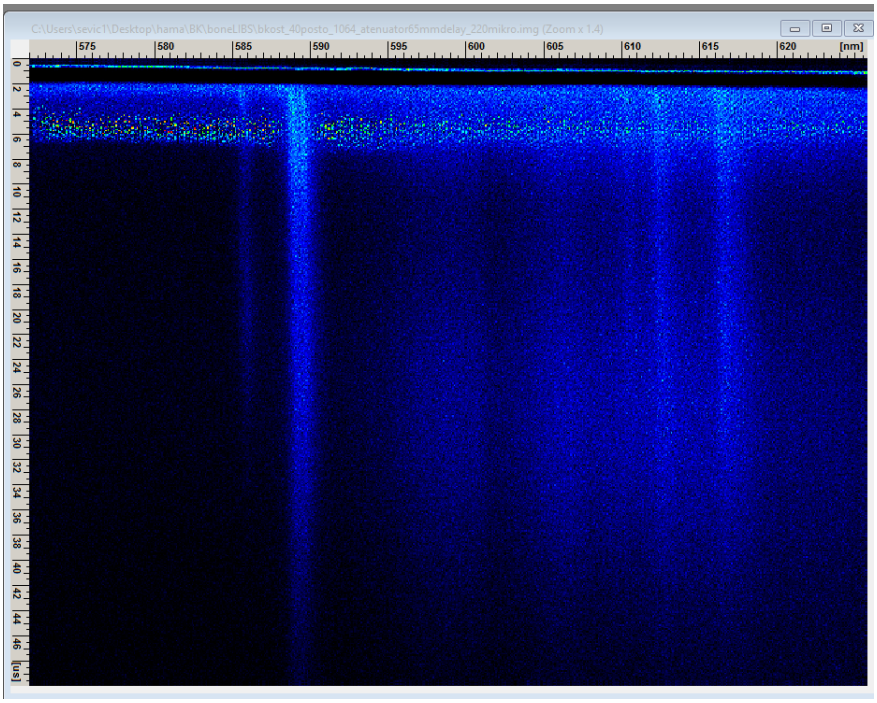

Figure 1: Streak image of LIBS of a dry bone.

materials, but for printed circuit board) presented in [5]. The real application would be based on using the simpler, not time resolved spectrograph with gated acquisition time frame. Our analysis of streak images provides the proof of the concept. Also, the optimal value of gate time is determined by our analysis.

[1] R.K. Gill *et al.*, J. J. Biophotonics **9** (2016) 17.
[2] B. Cencic *et al.*, Appl. Phys. A **112** (2013) 65.
[3] G. Hawlina *et al.*, BMC Ophthalmology **14** (2014) 131.
[4] M.S. Rabasovic *et al.*, IEEE Trans. Plasma Sci. **42** (2014) 2588.
[5] M.S. Rabasovic *et al.*, Appl. Phys. A, **122** (2016) 186.

Ejected electron spectra from Coster-Kroning transitions in argon

B.P. Marinković[1], J.J. Jureta[1], L. Avaldi[2]

[1]*Laboratory for Atomic Collision Processes, Institute of Physics Belgrade, University of Belgrade, Pregrevica 118, 11080 Belgrade, Serbia*

[2]*CNR-Istituto di Struttura della Materia, Area della Ricerca di Roma 1, CP10, 00015 Monterotondo Scalo, Italy*

High resolution ejected electron spectroscopy has been used to investigate ejected electrons in the energy region of the Coster-Kronig (C-K) transitions from 25 to 56 eV in Ar at incident electron energies of 243, 324, 606, 909 and 2018 eV and fixed ejection angle of 90°. The C-K spectrum in Ar includes transitions from the initial state $1s^2 2s 2p^6 3s^2 3p^6$ to the final states $1s^2 2s^2 2p^5 3s(^1P,^3P)3p^6$, and $1s^2 2s^2 2p^5 3s^2 3p^5(^3D, ^1D, ^3S, ^1S)$ [1]. In the C-K process the vacancy in the 2s shell (L_1) made by the impact of electrons with energies larger than 327 eV is filled by an electron from the 2p subshells ($L_{2,3}$), while the second electron from either 3s or 3p subshells (M_1, $M_{2,3}$) is promoted to the continuum. The final result is formation of two separate groups of peaks around 30 and 50 eV i.e. (L_1-$L_{2,3}M_1$) and (L_1-$L_{2,3}M_{2,3}$) respectively.

The intensity evolution of all states in the C-K energy region was studied at several incident electron energies from 243 to 2018 eV. The calibration of ejected energy scale was made with respect to the energy position of the Ar $3d(^1D)$ state at 11.72 eV measured under the same experimental conditions.

The measurements have been carried out using a crossed electron-atom beam apparatus OHRHA [2] equipped with an electron gun that can be rotated around the axis of the electrostatic lenses of the analyzer, and the hemispherical analyzer with 7 channeltrons as detectors. The energy resolution of the ejected electron spectra measured as full width at half maximum (FWHM) of the narrowest feature in the spectrum, was typically between 60 and 80 meV.

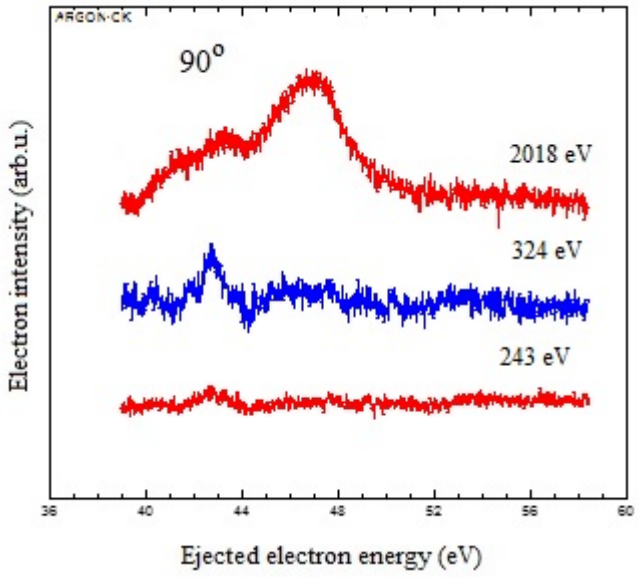

Figure 1: Coster – Kroning transition lines in Ar obtained at 243, 327 and 2018 eV incident electron energies and ejection angle of 90°.

[1] T. Kylli *et al.*, Phys. Rev. A **59** (1999) 4071.
[2] J.J.Jureta *et al.*, Int.J.Mass Spectrom. **114** (2014) 365.

Electron transmission through steel capillary

B.P. Marinković[1], M.Lj. Ranković[1], J.B. Maljković[1], A.R. Milosavljević[2], D. Borka[3], C. Lemell[4], K. Tökesi[5]

[1]*Institute of Physics Belgrade, University of Belgrade, Pregrevica 118, 11080 Belgrade, Serbia*

[2]*PLÉIADES beamline, Synchrotron SOLEIL, L'orme des Merisiers, Saint-Aubin - BP48, 91192 GIF-sur-YVETTE CEDEX, France*

[3]*Atomic Physics Laboratory, Vinča Institute of Nuclear Sciences, University of Belgrade, Belgrade, Serbia*

[4]*Institute for Theoretical Physics, Vienna University of Technology, Vienna, Austria*

[5]*Institute for Nuclear Research, Hungarian Academy of Sciences (ATOMKI), Debrecen, Hungary and ELI-ALPS, ELI-HU Non-profit Kft., Szeged, Hungary*

The transmission of low-energy electrons through platinum [1, 2] and steel capillaries have been investigated both experimentally and theoretically. The length of the present steel capillary was $L = 19.50$ mm while the inner diameter was $d = 0.90$ mm. Kinetic energy distribution of electrons transmitted through steel capillary was recorded at two tilt angles (the angle between the incident electron beam and the capillary axis) of 2.64° and 4.0°, respectively. The experimental results were obtained by an electron spectrometer which consists of an electron gun, a double cylindrical mirror energy analyzer (DCMA) and a channeltron detector.

Electron transmission is modelled by a classical trajectory Monte Carlo simulation taking both elastic and inelastic scattering events of primary electrons colliding with the inner wall of the capillary and transport of secondary electrons into account.

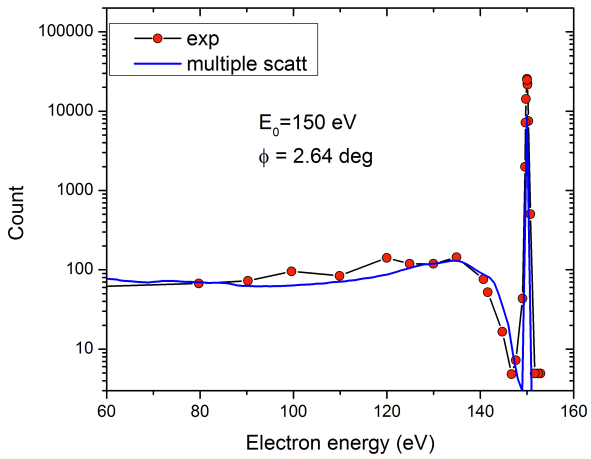

Figure 1: Energy spectra of electrons transmitted through a steel capillary.

Figure 1 shows energy spectra of 150 eV electrons passing through the steel capillary at 2.64° tilt angle. We found excellent agreement between our simulated electron-energy spectra with experimental data.

[1] A.R. Milosavljević *et al.*. Nucl. Instr. Meth. Phys. Res. B **354** (2015) 86.

[2] D. Borka *et al.*, Nucl. Instr. Meth. Phys. Res. B, in press (2017), http://dx.doi.org/10.1016/j.nimb.2017.02.024

Low energy electron attachment to C_3F_8, C_4F_8 molecules and clusters

D. Mészáros[1], P. Papp[1], Š. Matejčík[1]

[1]*Department of Experimental Physics, Faculty of Mathematics, Physics and Informatics, Comenius University in Bratislava, Mlynská dolina F2, Bratislava 84248, Slovakia*

Two different precursors C_4F_8 and C_3F_8 used in Plasma Enhanced Chemical Vapour Deposition (PECVD) as well as in the alternative Deep Reactive-Ion Etching (DRIE) spraying technology were studied. The electron attachment and dissociative electron attachment (DEA) of both molecules has been studied in the gas phase, the C_4F_8 in the clusters as well. In the gas phase mass spectrometric studies we have seen three common fragments for both measured molecules, F^-, CF_3^-, $C_2F_5^-$. For C_4F_8 the fragments F_2^-, CF_2^-, CF_3^- and $C_3F_5^-$ were found to be in excellent agreement with Harland's work [1], but recently measured over larger energy range and with additional resonances for F^-, F_2^-, CF_3^- and $C_3F_5^-$. New cross sections were obtained for DEA products $C_2F_3^-$, $C_2F_5^-$, $C_4F_7^-$, and for the molecular ion $C_4F_8^-$ with a strong resonance at ~ 0 eV.

In the cluster environment we have detected core exited resonances as well for the molecular ion of C_4F_8 which were not observed in the gas phase, these resonances became more significant with increasing size of the $(C_4F_8)_nC_4F_8^-$ cluster size. These are the dominant products of electron attachment of the C_4F_8 cluster spectrum, other significant products are formed via competitive reactions, formation of F^- and $(C_4F_8)_nF^-$ vs $C_4F_7^-$ and $(C_4F_8)_nC_4F_7^-$. Here the dominant resonance above 4 eV measured in the gas phase is strongly suppressed with the clusters. New ions have been observed in the monomolecular part of the cluster spectrum contrary to the gas phase spectrum of DEA to C_4F_8, namely $C_2F_4^-$, $C_3F_6^-$ and $C_4F_6^-$.

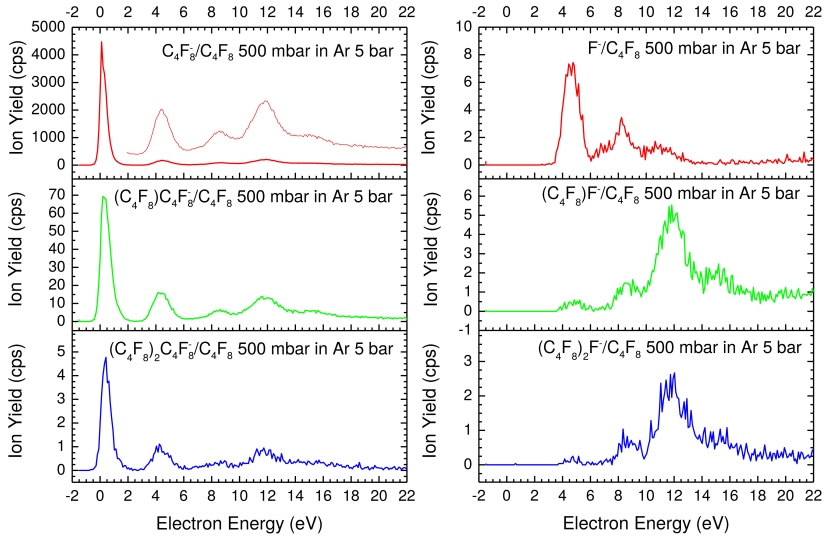

Figure 1: Dissociative electron attachment cross sections of $C_4F_8^-$, its dimer, trimer molecular clusters (left) and F^- with monomer and dimer cluster of C_4F_8 (right).

Financing of this work was by the Slovak Grant Agency VEGA 1/0417/15. This work was supported by the Slovak Research and Development Agency, project Nr. APVV-15-0580. This project has received funding from the European Union's Horizon 2020 research and innovation programme under grant agreement No 692335.

[1] P.W. Harland and J.C.J. Thynne, Int. J. of Mass Spectrom. Ion Phys. **10** (1972) 11.

PIXE induced by medium energy heavy ions in application to analysis of thin films and subsurface regions

M. Moneta[1], R. Brzozowski[2], M. Antoszewska-Moneta[1], E. Frątczak[1], B. Pawłowski[1]

[1]*Uniwersytet Łódzki, Katedra Fizyki Ciała Stałego, Pomorska 149, PL 90-236 Łódź, Poland*

[2]*Krajowe Centrum Ochrony Radiologicznej w Ochronie Zdrowia, Smugowa 6, 91-433 Łódź, Poland*

X-rays emitted during the impact of heavy ions on the surface provide not only information on atomic excitation and further recombination processes but also on elemental composition and dynamics of restructuring of the surface.

In this work characteristic radiation emitted during interaction of medium energy (240 keV) light and heavy ions (Ar) with Au/Si thin (10 Å) film and Au foils in various diffraction geometries were measured in order to analyse transitions between states with high quantum numbers, Fig. 1.

Also, the *X*-radiation generated in collisions of medium energy (220 keV) heavy ions (Ar,N) with Si surface and with Fe/Cu/Si thin (10 Åto 50 nm) films in grazing incident-exit angle geometry were measured in time sequence in order to determine dynamics of formation of implanted-sputtered subsurface region and in order to show that the dynamics of selective surface structure and composition modification during implantation can be studied with PIXE, Fig. 2.

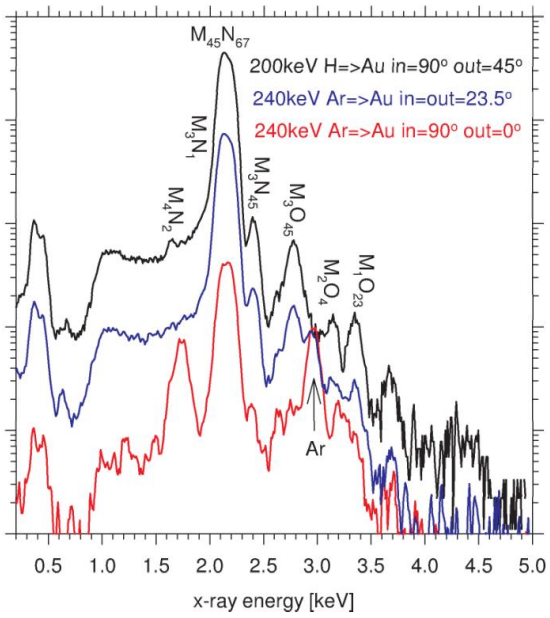

Figure 1: Raw PIXE spectra of Au M-lines.

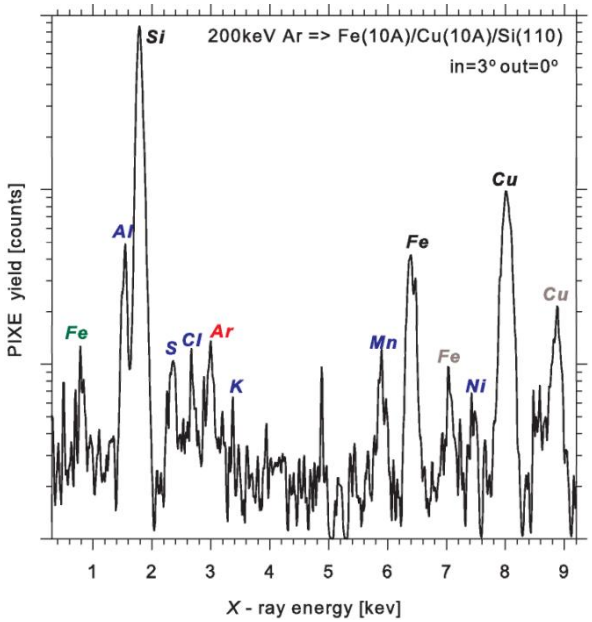

Figure 2: PIXE from Fe(10A)/Cu(10A)/Si(110).

[1] M. Antoszewska *et al.*, Nuclear Instr. Meth. Phys. Res. B **310** (2013) 27.
[2] M. Antoszewska-Moneta *et al.*, Eur.Phys. J. D **69** (2015) 77.

Photophysical and structural properties of quinoxalinophenanthrophenazines thin films

E. Frątczak[1], P. Uznański[2], B.R. Kaafarani[3], M. Moneta[1]

[1]*Faculty of Physics and Applied Informatics, University of Łódź, Łódź, Poland*

[2]*Centre of Molecular and Macromolecular Studies, Polish Academy of Sciences, Łódź, Poland*

[3]*Department of Chemistry, American University of Beirut, Beirut, Lebanon*

Thin films of beam deposited 2,11-bis(1,1-dimethylethyl)-6,7,15,16-tetramethyl quinoxalino[2',3':9,10] phenanthro[4,5-abc]phenazine (TQPP-Me) (Fig. 1a) were analysed in view of their microstructural and anisotropic optical properties. TQPP-Me film of 44 nm thickness was obtained by organic molecular beam deposition (OMBD) in ultra high vacuum conditions onto silicon/native silica (Si/SiO_2), quartz and glass substrates. The alignment of TQPP-Me molecules in the formed films was studied by optical polarized microscopy, atomic force microscopy (AFM), FTIR in transmission and reflection modes, by UV-Vis absorption and fluorescence spectroscopy with polarized light and spectroscopic ellipsometry.

The purpose of our studies was to demonstrate how anisotropy and molecular ordering of TQPP-Me affects the optical and electronic properties of thin films. Anisotropic optical properties and morphology of studied films exhibit continuous texture with strongly uniaxial anisotropy, with the molecule long axis oriented parallel to the surface [1]. Morphological features of the film deposited on Si/SiO_2 substrate were observed using tapping mode of AFM in a height and phase contrast. In AFM images crystalline structures with needle-like shape are discernible with needles grouped in domains (Fig. 1b). The films are uniform as is evident from optical microscope examinations taken in crossed polarizers of deposited TQPP-Me film on glass substrate, where total extinction was observed independent of azimuthal direction indicating uniaxial alignment [1].

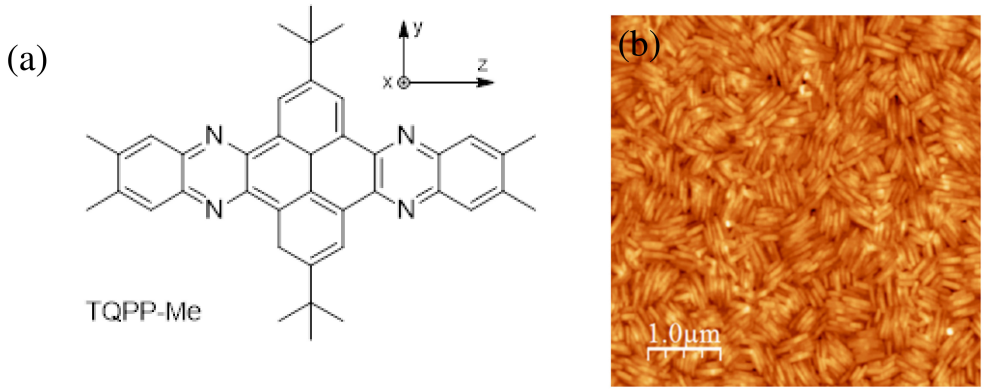

Figure 1: Chemical structure of TQPP-Me (a). AFM topography image of TQPP-Me surface morphology on Si/SiO_2 substrate (b).

In this work the assignment of the infrared vibrations obtained in GATR measurements in non-polarized light was performed by comparison with microcrystalline powder detected by diamond-ATR technique. The sample is anisotropic with uniaxially distributed molecules on Si/SiO_2 surface (vide infra) whereas the powder composes of randomly oriented microcrystals [1]. In the GATR measurements with p- and s-polarized IR radiation only those modes are observed which have non-zero components of transition dipole moments parallel or perpendicular to the plane of light incidence [2]. Two types of spectra were analyzed: ATR for powdered crystalline sample and p- and s- polarized GATR. The spectrum of powdered molecules is similar to spectrum of the film in s-polarized direction. Comparing p- and s-polarized spectra it is seen that most of the peaks of s-polarized spectrum is intensified prior to p-polarized spectrum. The ranges of attenuation of the intensities of the maxima probably correspond to the transitions along y

axes of the molecules, assigning x, y and z axes to the molecules corresponding to their short, long and perpendicular to the molecular plane axes [1]. The similarity of the s- spectrum to the powdered spectrum and the difference between p- and s- spectra suggests that the molecules are arranged with their long axes along the substrate surface with their short axes perpendicular to the substrate with uniaxial alignment (Fig. 2) [1].

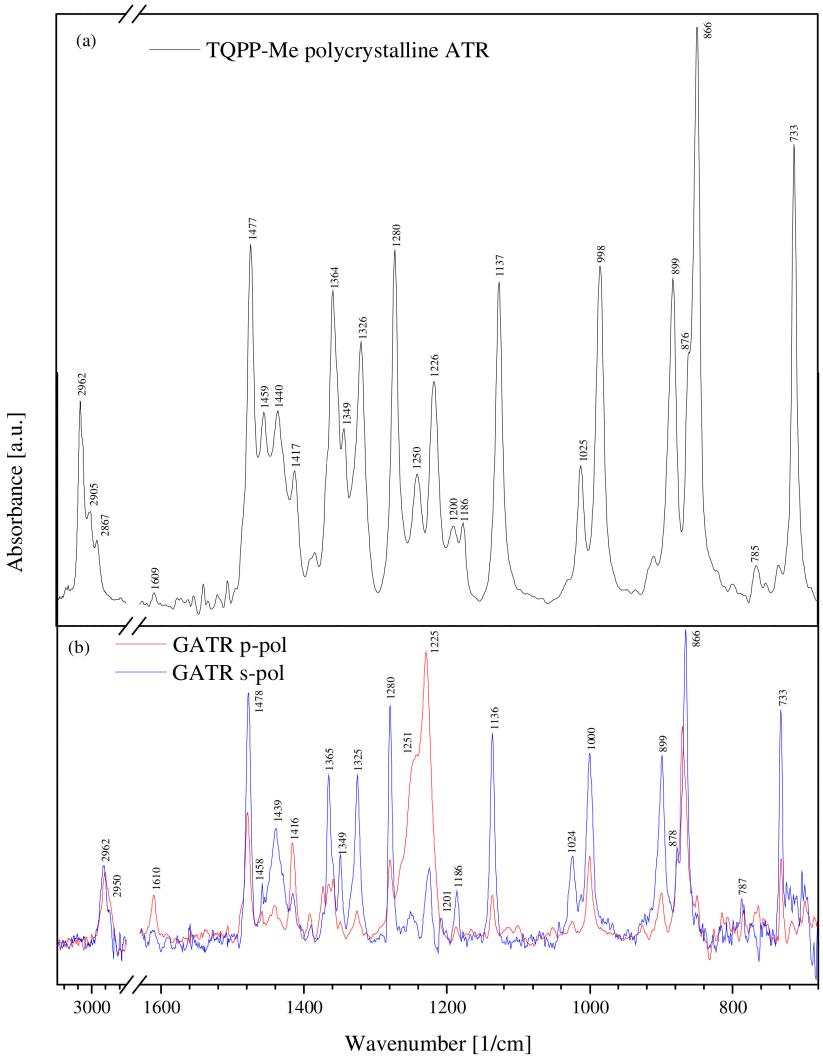

Figure 2: Comparison of the infrared powdered spectrum with its 44-nm thick film spectra. The upper curve (a) presents the ATR spectrum of polycrystalline powder. The lower curves (b) show a grazing angle GATR spectra of p-polarized light (red line) and s-polarized light (blue line).

Optical properties were further studied using spectroscopic ellipsometry. The experimental data were calculated using generalized VASE model of complex dielectric functions (DF). For modelling electron-vibrational progression a Lorentzian oscillator was used, already successfully applied in deconvolution of the visible absorption spectrum. Fig. 3 shows the resulting complex refractive index and extinction coefficient in plane and out of plane of the substrate as a function of the energy. For the refractive index n (Fig. 3a) the highest anisotropy is detected in the in-plane. The out-of-plane index lies below and is less featured. Under our experimental conditions absorption for the perpendicular component of dielectric functions is probably smaller, and this finding is in agreement with the orientation of TQPP-Me molecules on native silica with their short axis being close to the surface normal. The extinction coefficient k in the substrate plane in Fig. 3b has similar characteristic as the refractive index with the difference of intensities of the maxima. The maxima of the out-of-plane component are slightly shifted. Spectra from Fig. 3a and Fig. 3b are compared to their UV-VIS spectra of a layer and solution in Fig. 3c.

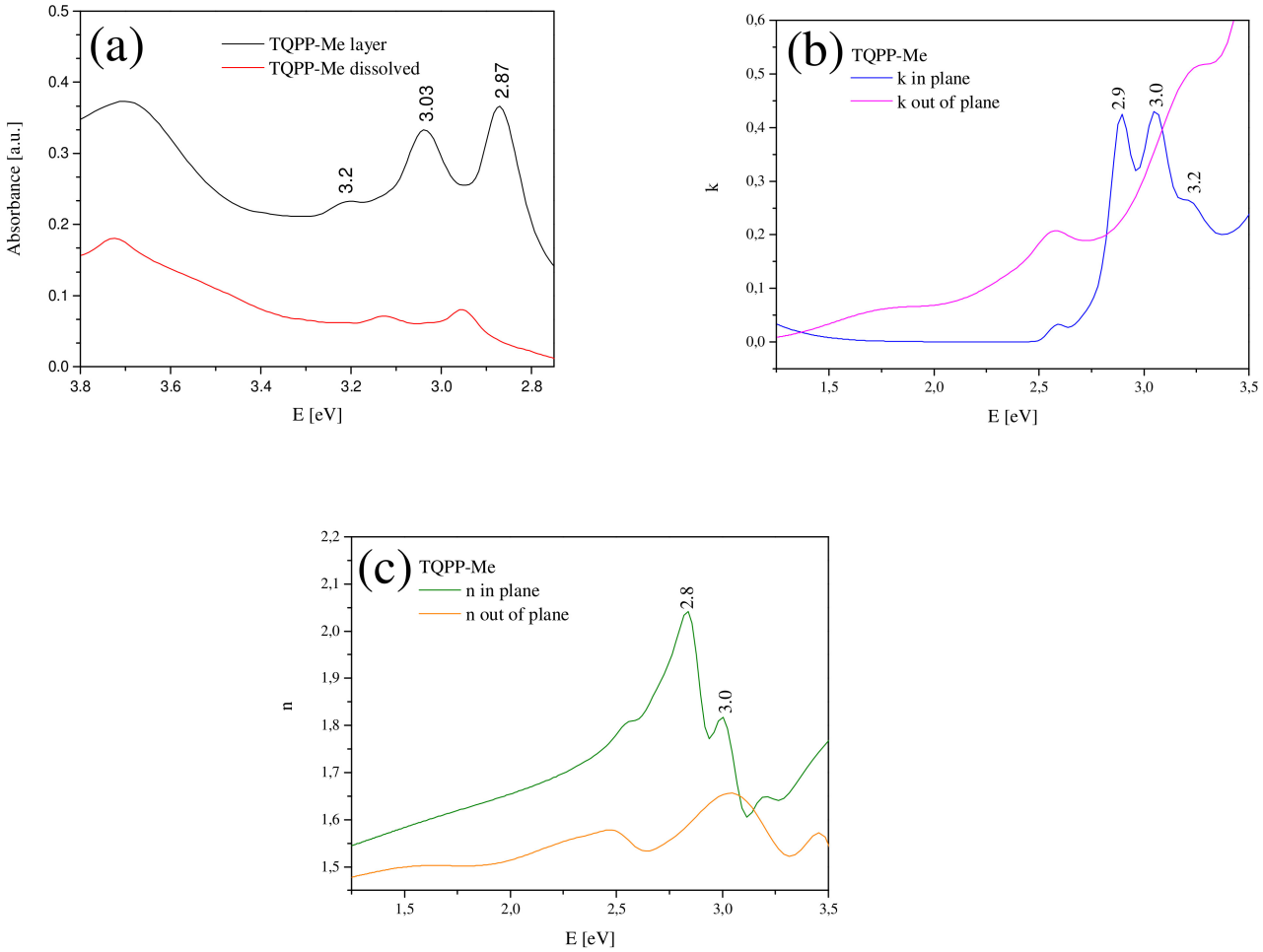

Figure 3: Ellipsometric spectra of TQPP-Me: in-plane and out-of-plane components of refractive index n in (a) and extinction coefficient k in (b). UV-Vis spectra of TQPP-Me layer and its toluene dilution (c).

[1] E.Z. Frątczak *et al.*, Chem. Phys. **456** (2015) 49.
[2] M. Milosevic *et al.*, Appl. Spectrosc. **57** (2003) 724.

High resolution study of the autoionizing states of He in the vicinity of the equal velocity region

B. Paripás[1], J.J. Jureta[2], B. Palásthy[1], B.P. Marinković[2], G. Pszota[1]

[1]*Institute of Physics, University of Miskolc, 3515 Miskolc-Egyetemváros, Hungary*

[2]*Laboratory for Atomic Collision Processes, Institute of Physics Belgrade, University of Belgrade, Pregrevica 118, 11080 Belgrade, Serbia*

By "equal velocity region" we mean the primary electron energy range in which the energies of the autoionizing electrons approximately match that of the scattered electrons. This range is around 90-95 eV for the four most important autoionizing states of helium. Then such interesting phenomena can occur as the post-collision interaction and certain types of the state-to-state interference. We have been studying this range for a long time [1], concentrating the interference of the $2s^2(^1S)$ and $2p^2(^1D)$ resonances. It takes place at 93.15 eV critical primary energy, where the energy of the scattered electron from one reaction path equals the energy of the ejected (autoionizing) electron released along the other path and vice versa: here the scattered-ejected electron pairs are indistinguishable. The observation of this exchange interference is disturbed by the Fano interference (the interference between the direct and indirect ionization), too, which occurs at all primary energies. We intend to study it separately in the neighbourhood of the critical energy, and then to estimate its measure for the critical energy.

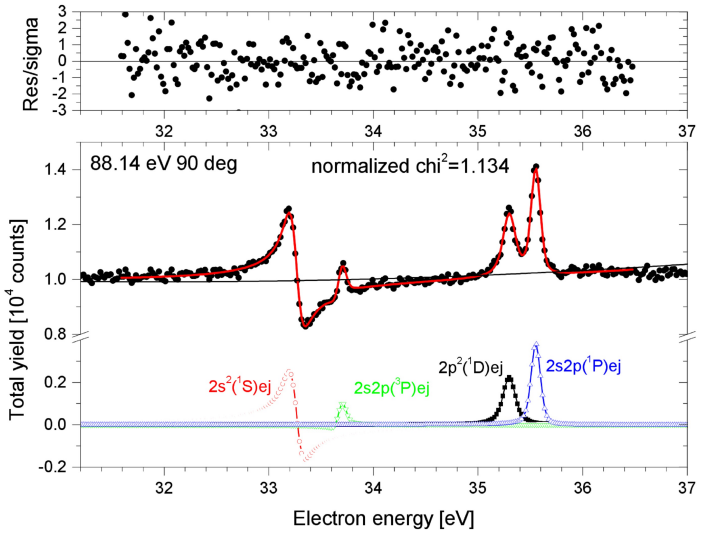

Figure 1: The electron spectrum measured at 90° ejection angle at 88.14 eV primary energy with the best computer fit (solid line). At the bottom the spectrum components, at the top the residuals (in sigma units) are shown.

The present measurements were made by an Omicron High Resolution Hemi-spherical Analyzer (OHRHA) [2] at 88 eV and 97 eV primary energies (where the groups of the ejected and the scattered electron peaks are well separated), at 130°, 90° and 50° ejection angles. The measured spectra were evaluated by a computer code, using the Shore parametrization.

[1] B. Paripás *et al.*, Eur. Phys. J. D **69** (2015) 34.
[2] J.J. Jureta *et al.*, Int. J. Mass Spectr. **114** (2014) 365.

Classical Trajectory Monte Carlo simulation of coincidence experiments in electron impact ionization of helium

B. Paripás[1], B. Palásthy[1], K. Tőkési[2,3]

[1]*Institute of Physics, University of Miskolc, 3515 Miskolc-Egyetemváros, Hungary*

[2]*Institute for Nuclear Research of HAS (Atomki), 4026 Debrecen Bem tér 18/c, Hungary*

[3]*ELI-ALPS, ELI-HU Non-profit Ltd., Dugonics tér 13, H-6720 Szeged, Hungary*

The possible state-to-state interferences of the $2s^2(^1S)$ and $2p^2(^1D)$ autoionizing resonances of He [1] are considered. These states decay to the same He^+1s^{-1} final state, the energies of the ejected autoionizing electrons are 33.24 eV and 35.32 eV, respectively. The critical energy, where the state-to-state interference can occur is 93.15 eV. At this primary energy the energy of the scattered electron from one reaction path equals the energy of the ejected electron released along the other path and vice versa.

This effect was previously studied by our cylindrical mirror analyser system (Fig. 1) both in coincidence [2] and in non-coincidence [3] experiments. The observation of this exchange interference is essentially disturbed by the background of direct ionization and its interference with the indirect ionization (Fano interference). Thus the possibility of the observation of the state-to-state interference is greater in the regions where the yield of direct process is smaller.

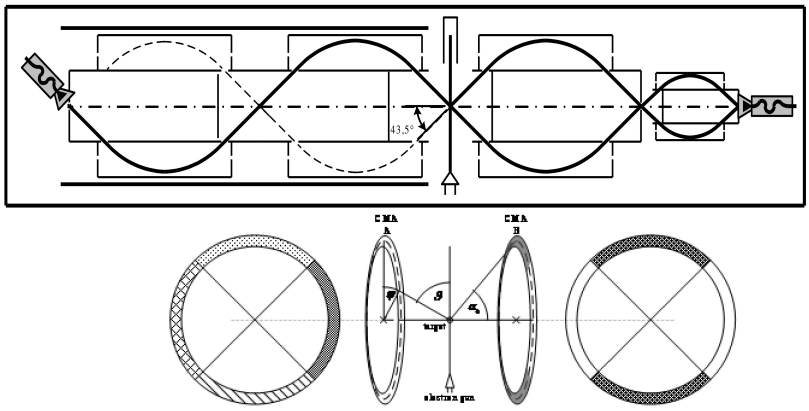

Figure 1: The sketch and entrance geometry of our $(e, 2e)$ coincidence spectrometer system.

To mimic the experimental observation we performed four-body classical trajectory Monte Carlo calculations [4]. In our model the projectile is one particle (electron) and the target contains three particles, the helium core and two electrons. The binding energies of the target electrons to the target core are 0.903 a.u. and 2 a.u. according to the first and second ionization energy of helium. In the present case, all interactions among the particles are the pure Coulomb interactions except the interaction between the two target electrons. To avoid spontaneous autoionization this interaction is completely neglected during the calculations.

We calculated the yields of non-coincidence and coincidence events detected in various combinations of sectors showing in Fig 1. Our calculations justify the experimental observations.

[1] J.P.V. den Brink *et al.*, J. Phys. B **22** (1989) 3501.
[2] B. Paripás *et al.*, Eur. Phys. J. D **69** (2015) 34.
[3] B. Paripás *et al.*, J. Phys. B **369** (2016) 34.
[4] Tőkési K *et al.*, Eur. Phys. J. D **68** (2014) 255.

VUV action spectroscopy of protonated Tri-Alanine peptide

M. Ranković[1], A. Milosavljević[2], A. Giuliani[3],F. Canon[4] and Laurent Nahon[2]

[1]*Institute of Physics Belgrade, Pregrevica 118, 11080 Belgrade, Serbia*

[2]*SOLEIL, l'Orme des Merisiers BP48, 91192, Paris, France*

[3]*INRA, Rue de la Géraudiére BP 71627, 44316, Nantes, France*

[4]*CNRS, Boulevard Jeanne d'Arc 9E, F-21000, Dijon, France*

The studies of interaction of energetic photons with big macromolecules such as amino acids, peptides and proteins in the gas phase have become accessible in recent years with developments of electrospray (ESI) and mass spectrometry techniques. A wide photon energy range and high flux provided by synchrotron radiation sources in combination with these techniques gives one a very powerful tool [1] for closer investigation of radiation damage at molecular level.

We present the photodisociation results of protonated small peptide Tri-Alanine obtained at VUV beamline DESIRS of synchrotron SOLEIL near Paris, France. The experiment was performed by coupling the beamline with quadrupole ion trap mass spectrometer [2]. Electrosprayed cation precursor $[AAA+H]^+$ was selected in the ion trap and subjected to VUV photons of (6.7-9.7) eV energy range.

The backbone fragments corresponding to the peptide bond scision are visible, although neutral losses dominate the mass spectrum Fig 1. Weak energy band at about 7 eV was observed for some backbone ion yields. Moreover, ion yields from almost all fragments show strong increase after 9 eV, suggesting another energy band. For small peptides, these bands might be traced to $\pi\pi^*$ transitions as previously observed [3].

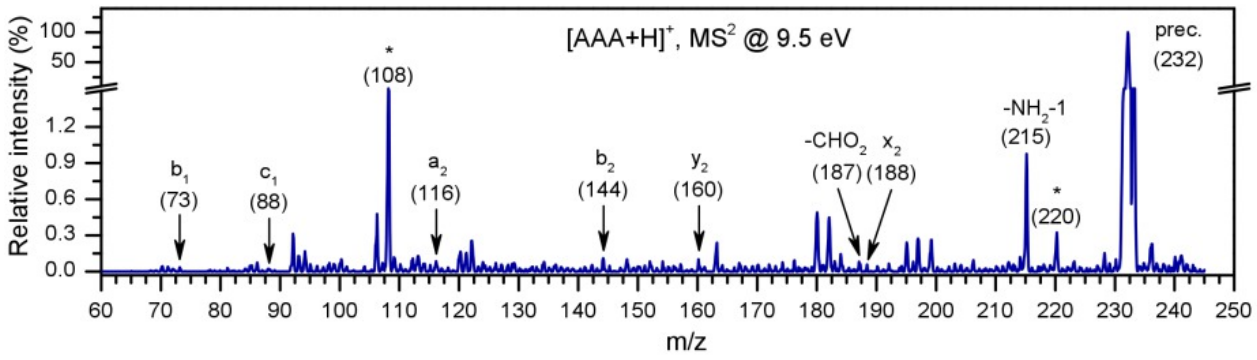

Figure 1: Tandem mass spectrum of protonated AAA peptide recorded at 9.5 eV.

Acknowledgements. This work was supported by the French ANR (project no. ANR-08-BLAN-0065), the "Pavle Savic" bilateral scientific project between Serbia and France (No. 27482TE) and the COST Action MP1002 (Nano-IBCT). A.R.M. and M.Lj.R., acknowledge support by the Ministry of Education, Science and Technological Development of the Republic of Serbia under project 171020. We are grateful to the SOLEIL general staff for providing beamtime under project no. 20120874 and 20130388.

[1] A. Giuliani *et al.*, Mass Spectrom. Rev. **33** (2014) 424.
[2] A.R. Milosavljević *et al.*, Angew. Chem.-Int. Edit. **52** (2013) 7286.
[3] M. Lj. Ranković *et al.*, J. Chem. Phys. **143** (2015) 244311, 1-8.

Radiative double electron capture in $F^{9+}+N_2$ and Ne collisions

J.A. Tanis[1], P.N.S. Kumara[1], D.S. La Mantia[1], P.M. Niraula[1], S. Iqbal[1], M.C. Bridges[1], A. Simon[2], A. Kayani[1]

[1]*Western Michigan University, Department of Physics, Kalamazoo, Michigan 49008 USA*

[2]*University of Notre Dame, Department of Physics, Notre Dame, Indiana 46556 USA*

Radiative double electron capture (RDEC), which occurs when two electrons from a target are captured by a projectile with the simultaneous emission of a single photon, is being investigated for fully-stripped projectiles colliding with gaseous targets. The process is essentially the inverse process of double photoionization, and consequentially involves electron correlation. RDEC is similar to the well-known process of one-electron radiative electron capture (REC). In previous experiments [1–3] done at GSI for high-energy projectiles incident on both gas and thin-foil targets, evidence for RDEC could not be identified. The first successful measurements were done at WMU for lower energy 38 MeV O^{8+} [4] and 42 MeV F^{9+} [5] projectiles on thin-foil carbon targets, giving cross sections nearly two orders of magnitude larger than theoretical predictions [6]. However, the analysis was complicated by additional charge changing in the thin-foil target causing RDEC to also appear in the Q-1 channel.

In the present measurements, done at Western Michigan University using the tandem Van de Graaff accelerator, a beam of 40 MeV F^{9+} ions collided with N_2 and Ne targets in a differentially pumped cell. A Si(Li) detector placed at 90° to the beamline detected emitted x rays. The ion beam was subsequently analyzed with a dipole magnet and the charge states Q-1 and Q-2 were detected with individual silicon detectors.

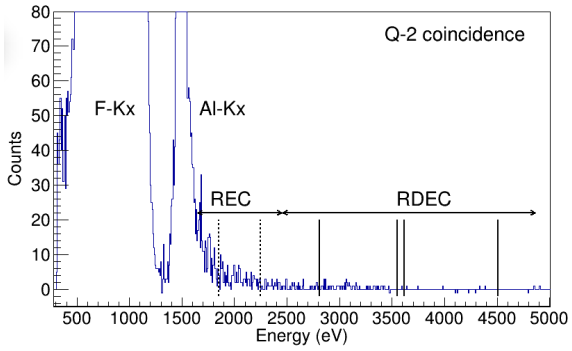

Figure 1: X rays coincident with double capture (Q-2) for 40 MeV $F^{9+} + N_2$. Calculated line positions for REC (K→K and valence→K transitions, respectively) are shown as broken vertical lines and for RDEC (KK→KL, KK→KK, valence-valence→KL and valence-valence→KK transitions, respectively) as solid vertical lines. The lines are broadened by the Compton profile of the target electrons.

Figure 1 shows a preliminary spectrum for x rays coincident with double capture (Q-2) for 40 MeV $F^{9+} + N_2$. Expected REC and RDEC photon energies for the projectile-target system are indicated. These energies are broadened by the Compton profile of the target electrons captured. The counts observed in the RDEC region correspond to an upper limit cross section of about 1 b, which is approximately an order of magnitude larger than predicted in Ref. [6]. Additional data are required and further analysis will be performed.

[1] A. Warczak *et al.*, Nucl. Instrum. Methods Phys. Res. B **98** (1995) 303.
[2] G. Bednarz *et al.*, Nucl. Instrum. Methods Phys. Res. B **205** (2003) 573.
[3] N. Winters *et al.*, Phys. Scr. T **156** (2013) 014048.
[4] A. Simon *et al.*, Phys. Rev. Lett. **104** (2010) 123001.
[5] T. Elkafrawy *et al.*, Phys. Rev. A **94** (2016) 042705.
[6] E. A. Mistonova and O. Yu. Andreev, Phys. Rev. A **87** (2013) 034702.

The photofragmentation of the core excited halothane molecule

S.D. Tošić[1], M. Radibratović[2], M. Milčić[3], P. Bolognesi[4], L. Avaldi[4], R. Richter[5], M. Coreno[4,5], B.P. Marinković[1]

[1]*Institute of Physics Belgrade, University of Belgrade, Pregrevica 118, 11080 Belgrade, Serbia*

[2]*Institute of Chemistry, Technology and Metallurgy – Center for Chemistry, University of Belgrade, Njegoúseva 12, 11000 Belgrade, Serbia*

[3]*University of Belgrade, Faculty of Chemistry, Studentski trg 16, Belgrade, Serbia*

[4]*Istituto di Struttura della Materia-CNR (ISM-CNR), Area della Ricerca di Roma 1, Monterotondo Scalo, Italy*

[5]*Elettra-Sincrotrone Trieste, Area Science Park, I-34012 Basovizza, Trieste, Italy*

In recent years, great attention has been paid to halogenated anesthetics and their role in the destruction of the earth's ozone layer [1]. One of the most commonly used is halothane ($C_2HBrClF_3$). Compared to the other volatile anestethics from the same group (halogenated chlorofluorocarbons) this bromide-containing agent is the most destructive against ozone.

We present both experimental and theoretical results related to the photofragmentation of the core-excited halothane molecule. The experiments have been performed at the Gas Phase photoemission beamline of the Elettra synchrotron radiation source (Trieste, Italy) using photons near the C 1s ionization edge ($\sim$ 300 eV). The mass spectrum [as shown in Fig.1] is dominated by lighter mass fragments.

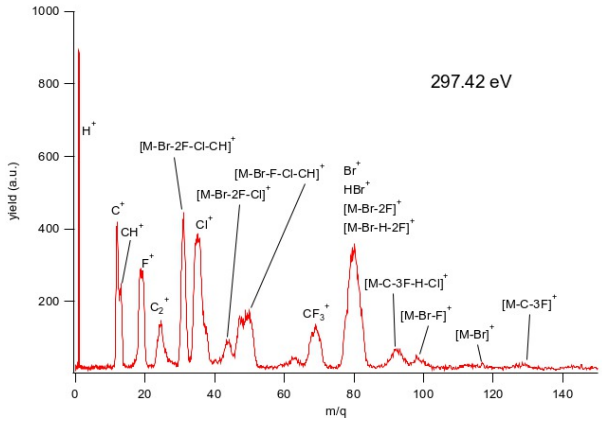

Figure 1: The fragmentation mass spectra of halothane.

To explain the observed large number of lighter mass fragments extensive molecular dynamics (MD) simulations of $C_2HBrClF_3^{2+}$ ion at different temperatures were performed. All MD simulations were carried out in the microcanonical (NVE) ensemble using Verlet algorithm for time integration. At each step of the simulation the potential energy was calculated by minimizing the electronic energy with self-consistent charge-density-functional tight-binding (SCC-DFTB) method as implemented in the DFTB+ code [2]. The results of MD simulations have confirmed the experimental findings: there are fragmentation paths producing almost all fragments found in the mass spectra. For the main fragmentation pathways the minima and the transition states on the potential energy surface were calculated with more accurate quantum chemical methods.

Work partially supported by the MAECI Serbia–Italy Joint Research Project "A nanoview of radiation-biomatter interaction" and the MESTDRS (OI 171020, OI 172065).

[1] A.C. Brown *et al.*, Nature **341** (1989) 635.
[2] B. Aradi *et al.*, J. Phys. Chem. A **111** (2007) 5678.

List of Participants

Václav Alt
Charles University
Prague, Czech Republic
alt.vaclav@gmail.com

Ticia Buhr
Justus-Liebig-Universität
Gießen, Germany
ticia.buhr@physik.uni-giessen.de

Martin Čížek
Charles University
Prague, Czech Republic
Martin.Cizek@mff.cuni.cz

Marián Danko
Comenius University
Bratislava, Slovakia
mdanko@centrum.sk

Petr Dohnal
Charles University
Prague, Czech Republic
pr.dohnal@seznam.cz

Robert DuBois
Missouri University of Science and Technology
Rolla, Missouri, United States
dubois@mst.edu

Gustavo García
Institute of Fundamental Physics
Madrid, Spain
g.garcia@csic.es

Jiří Horáček
Charles University
Prague, Czech Republic
jiho@matfyz.cz

Dávid Hvizdoš
J. Heyrovský Inst. of Physical Chemistry
Prague, Czech Republic
hvizdosdavid@yahoo.co.uk

Jaroslav Kočíšek
J. Heyrovský Inst. of Physical Chemistry
Prague, Czech Republic
jaroslav.kocisek@jh-inst.cas.cz

Paola Bolognesi
CNR-Institute of Structure of Matter
Monterotondo, Italy
paola.bolognesi@cnr.it

Andrej Bunjac
University of Belgrade, Inst. of Physics
Belgrade, Serbia
bunjac@ipb.ac.rs

Roman Čurík
J. Heyrovský Inst. of Physical Chemistry
Prague, Czech Republic
roman.curik@jh-inst.cas.cz

Sándor Demes
Inst. for Nuclear Research (Atomki)
Debrecen, Hungary
demes.sandor@atomki.mta.hu

Alicja Domaracka
CIMAP
Caen, France
domaracka@ganil.fr

François Frémont
University of Caen
Caen, France
francois.fremont@ensicaen.fr

Alexei Grum-Grzhimailo
Lomonosov Moscow State University
Moscow, Russian Federation
algrgr1492@yahoo.com

Karel Houfek
Charles University
Prague, Czech Republic
karel.houfek@mff.cuni.cz

Zoltán Juhász
Inst. for Nuclear Research (Atomki)
Debrecen, Hungary
zjuhasz@atomki.hu

Janina Kopyra
Siedlce University
Siedlce, Poland
kopyra@uph.edu.pl

Sándor Kovács
Inst. for Nuclear Research (Atomki)
Debrecen, Hungary
kovacs.sandor@atomki.mta.hu

Bratislav Marinković
University of Belgrade, Inst. of Physics
Belgrade, Serbia
bratislav.marinkovic@ipb.ac.rs

Nigel Mason
The Open University
Milton Keynes, United Kingdom
nigel.mason@open.ac.uk

Dušan Mészáros
Comenius University
Bratislava, Slovakia
meszaros44@uniba.sk

Béla Paripás
University of Miskolc
Miskolc, Hungary
fizpari@uni-miskolc.hu

Sándor Ricz
Inst. for Nuclear Research (Atomki)
Debrecen, Hungary
ricz@atomki.hu

Viorica Stancalie
National Inst. for Laser, Plasma
and Radiation Physics
Bucharest, Romania
viorica.stancalie@inflpr.ro

Béla Sulik
Inst. for Nuclear Research (Atomki)
Debrecen, Hungary
sulik@atomki.mta.hu

Michal Tarana
J. Heyrovský Inst. of Physical Chemistry
Prague, Czech Republic
michal.tarana@jh-inst.cas.cz

Petra Votavová
Charles University
Prague, Czech Republic
afar@email.cz

Paulo Limão-Vieira
Universidade NOVA de Lisboa
Lisbon, Portugal
plimaovieira@fct.unl.pt

Fernando Martín
Autonomous University of Madrid
Madrid, Spain
fernando.martin@uam.es

Štefan Matejčík
Comenius University
Bratislava, Slovakia
Stefan.Matejcik@fmph.uniba.sk

Marek Moneta
University of Łódź
Łódź, Poland
alef_00@interia.pl

Miloš Ranković
J. Heyrovský Inst. of Physical Chemistry
Prague, Czech Republic
milos.rankovic@jh-inst.cas.cz

Jeff Shinpaugh
East Carolina University
Greenville, North Carolina, United States
shinpaughj@ecu.edu

Nikolaus Stolterfoht
Helmholtz-Zentrum Berlin
Berlin, Germany
nico@stolterfoht.com

John Tanis
Western Michigan University
Kalamazoo, Michigan, United States
john.tanis@wmich.edu

Sanja Tošić
University of Belgrade, Inst. of Physics
Belgrade, Serbia
seka@ipb.ac.rs

Programme

	Sunday 03/09	Monday 04/09	Tuesday 05/09	Wednesday 06/09
09:00 – 09:45		F. Martín	A. Domaracka	J. Kopyra
09:45 – 10:10		T. Buhr	S. Kovács	M. Danko
10:10 – 10:40		Coffee Break	Coffee Break	Coffee Break
10:40 – 11:25		P. Bolognesi	J. Shinpaugh	P. Limão-Vieira
11:25 – 11:50		A. Grum-Grzhimailo	F. Frémont	J. Kočíšek
11:50 – 12:15		Andrej Bunjac	N. Stolterfoht	N. Mason
12:15 – 14:00		Lunch	Lunch	Lunch
14:00 – 14:25		P. Dohnal		Departures
14:25 – 14:50		R. Čurík		
14:50 – 15:15	Registration	P. Votavová	Departure to Prague and excursion	
15:15 – 15:40		V. Stancalie		
15:40 – 16:15		Coffee Break		
16:15 – 19:00		Poster Sesssion ISC meeting		
19:00 –	Welcome reception	Individual dinner	Conference Dinner	